scientific reports

Check for updates

OPEN

Dual-antigen AdV5 vaccines against Crimean-Congo hemorrhagic fever virus induce superior humoral and Th1-biased cellular immunity

Alireza Hanifehnezhad[1,2,12], Sidika Oztop[3,12], Ece Tavukcuoglu[4], Yigit Tanyeri[5], Ekimcan Yoyler[6], Gokcen Gokce Tepeli[7], Nilay Unal[2], Asuman Bozkir[8], M. Taner Karaoglu[1], Gunes Esendagli[4], Ates Kara[9,10], Hakan Gurdal[11]✉ & Aykut Ozkul[1]✉

Platforms based on adenoviral vectors have proven their efficiency in developing vaccines and therefore can be considered potential candidates for immunization strategies against CCHFV. In this study, four replication-deficient recombinant human adenovirus serotype 5 (AdV5) vectors were engineered to express CCHFV antigens: a dual-antigen NP-P2A-Gc construct and monocistronic constructs for nucleoprotein (NP), glycoprotein complex precursor (GPC), and mature glycoprotein (Gc). Following GMP-compatible production and purification, vaccine candidates were evaluated in BALB/c mice ($n = 4$ per group) for immunogenicity and in IFNAR$^{-/-}$ mice ($n = 4$ per group) for protective efficacy using antigenically homologous or heterologous prime-boost regimens. Animals received priming immunization on day 0 and booster on day 28 followed by lethal CCHFV challenge (1000 $TCID_{50}$) on day 42. Immune responses were characterized via ELISA, virus neutralization tests, cytokine profiling, ELISpot, and flow cytometry. Post-challenge survival, viral loads in target organs, and safety profiles were assessed. All AdV5 constructs successfully expressed the target antigens and induced rapid seroconversion, with 75–100% of animals exhibiting antibody responses after priming with a single dose. The dual-antigen formulations elicited the strongest Th1-polarized responses particularly nucleoprotein + Gc combinations with interferon-γ production more than 30-fold above baseline and preferential expansion of $CD4^+$ T helper cells (60–70% of $CD3^+$ populations). Neutralizing antibody titers varied across groups (80–160 arbitrary units in high responders) but did not directly correlate with survival outcomes. After lethal challenge, multiple vaccine formulations achieved 100% survival throughout the 10-day observation period, while only control groups showed no protection. All vaccinated animals demonstrated significant viral load reduction of two to four logs in liver and spleen tissues, with some achieving complete clearance of the virus. Furthermore, no off-target vector dissemination was detected in examined tissues confirming safety profile of the constructs. Immunization with adenovirus serotype 5 (AdV5) vectors expressing CCHFV antigens elicited potent humoral and cellular immune responses, conferring 100% protection against lethal viral challenge

across the majority of evaluated formulations. Sterilizing immunity was observed in some animals, along with evidence that protection operates through multiple immune mechanisms including both neutralizing and non-neutralizing antibody-mediated pathways. These results strongly support further clinical development of AdV5-based CCHFV vaccines, with multiple formulation strategies showing high efficacy and providing flexibility for clinical advancement. GMP-compatible production methods have been successfully implemented for these candidates, supporting their advancement toward non-human primate studies and Phase I clinical trials.

Keywords Crimean-Congo hemorrhagic fever, Dual-antigen Adenovirus vector vaccine, Antigenically Homologous and Heterologous Prime-boost immunization, Neutralizing antibodies, Protective immunity

[1]Department of Virology, Faculty of Veterinary Medicine, Ankara University, Ankara 06070, Turkey. [2]Dollvet Biotechnology, Sanliurfa 63200, Turkey. [3]Department of Medical Biology, Faculty of Medicine, Ankara Medipol University, Ankara 06570, Turkey. [4]Department of Basic Oncology, Cancer Institute, Hacettepe University, Ankara 06100, Turkey. [5]Aziz Sancar Research Centre, Health Institutes of Turkiye, Ankara 06270, Turkey. [6]Graduate School for Health Sciences, Ankara University, Ankara 06070, Turkey. [7]Department of Histology and Embryology, Faculty of Medicine, Aydin Adnan Menderes University, Aydin 09070, Turkey. [8]Department of Pharmaceutical Technology, Faculty of Pharmacy, Ankara University, Ankara 06560, Turkey. [9]Department of Pediatrics, Pediatric Infectious Diseases Unit, Faculty of Medicine, Hacettepe University, Ankara06100, Turkey. [10]Vaccine Institute, Health Institutes of Turkiye, Istanbul 34718, Turkey. [11]Department of Medical Pharmacology, Faculty of Medicine, Ankara University, Ankara 06230, Turkey. [12]Alireza Hanifehnezhad and Sidika Oztop have contributed equally to this works and share first authorship. ✉email: hakan.gurdal@medicine.ankara.edu.tr; ozkul@ankara.edu.tr

Crimean-Congo hemorrhagic fever is an acute viral disease transmitted by ticks, caused by *Orthonairovirus haemorrhagiae*, which belongs to the *Nairoviridae* family within the *Bunyavirales* order[1]. Globally, this pathogen constitutes the most widespread tick-borne viral infection impacting human populations, with reported case fatality rates as high as 30% in certain areas. CCHFV is currently endemic across an extensive geographical distribution, including Africa, Asia, the Middle East, and Eastern Europe. Its recent appearance in the Iberian Peninsula underscores a concerning expansion of its geographic footprint and indicates a tendency for broader dissemination[2,3].

The clinical manifestations of CCHF can range from asymptomatic states to severe hemorrhagic disease with thrombocytopenia, elevated liver enzymes, and multi-organ failure[4]. Human transmission occurs primarily through the bites of infected Hyalomma ticks or via direct contact with the blood and tissues from infected livestock or human. The broad host range of CCHFV among domestic animals and wildlife combined with the extensive geographic distribution of competent tick vectors, makes disease control and prevention very difficult[5,6].

Although this virus has been researched intensively for many decades and poses a huge public health threat, there are currently no approved vaccines or specific therapeutic agents for human use against CCHFV[7]. This large gap in medical intervention has been repeatedly emphasized by the World Health Organization (WHO) in its Blueprint list as a priority disease under immediate research and development attention for CCHF[8]. Furthermore, an updated WHO research and development roadmap for CCHF in 2024 continues to highlight vaccine development as the most critical intervention priority in areas where the virus is endemic[9].

The nucleoprotein (NP) is the most abundant and highly conserved viral protein, playing essential roles in viral RNA packaging, replication, and transcription. Its high conservation across CCHFV strains makes it an attractive target for broad-spectrum vaccine development. The glycoprotein complex precursor (GPC) undergoes post-translational processing to generate mature Gc and Gn glycoproteins, which are the primary targets for neutralizing antibodies and mediate viral entry into host cells[1]. These functional roles explain why both antigens are critical components for comprehensive CCHFV vaccine strategies.

Vaccine development efforts against Crimean-Congo hemorrhagic fever have utilized a wide range of platform technologies such as inactivated virus vaccines, subunit vaccines, virus-like particles, DNA vaccines, and viral vector-based approaches[10,11]. Among these platforms, viral vector systems have shown great promise mainly because they can induce strong humoral and cellular immune responses. Early studies showed that nucleoprotein-only vaccines could protect animals[12,13]; but more recently it has become clear that glycoprotein complex is the main target for neutralizing antibodies and hence critical for optimal vaccine efficacy[14,15].

Adenoviral vector systems have been the most widely used systems in modern vaccine development against many pathogens, as evidenced by their success in COVID-19 vaccines[16]. On Crimean-Congo hemorrhagic fever virus, recent studies brought to light the potential of chimpanzee adenovirus vectors that have been modified to express CCHFV antigens. The ChAdOx2-vectored vaccine, which expresses CCHFV GPC and has entered Phase I clinical trials in August 2023, is a significant step forward since it is the first CCHFV vaccine tested on human subjects[17]. Additionally, human adenovirus type 5 vectors expressing NP have shown dose-dependent protective effects with prime-boost immunization strategies achieving up to 78% protection in interferon receptor knockout mouse models[13]. Both mRNA and DNA-based candidates also provided high levels of protection in different animal models including non-human primates and this was frequently observed without detectable neutralizing antibody titers thus highlighting the possibly crucial role of cellular immunity[12,18]. These findings complement the importance of neutralizing antibodies, demonstrating that CCHFV protection likely operates through multiple immune mechanisms including both humoral and cellular responses.

The advantages of Adenoviral vector platforms include a well-known safety record, strong immune responses after just one dose, better stability at higher temperatures than mRNA vaccines, and broad experience in

manufacturing[19–21]. There are still some challenges though like pre-existing immunity to common adenoviral serotypes and exactly optimizing antigen expression along with vector selection[21,22].

Recent comparisons of CCHFV vaccine candidates highlight how good dual-antigen strategies can be. Studies show that formulations including both NP and GPC antigens protect better than single-antigen approaches[23,24]. A major study published in eBioMedicine found that single-dose RNA vaccines co-expressing NP and GPC fully protected mice from lethal CCHFV infection. This shows the possible benefit of multi-antigen regimens[25]. Also, DNA vaccine studies in cynomolgus macaques found substantial protection with dual NP/GPC immunization protocols while individual antigen studies confirmed that NP could provide protective immunity on its own[23,24].

The choice of dual-antigen approaches is based on the different but complementary immune reactions triggered by different viral proteins. Although the glycoprotein complex is known to be the major target for neutralizing antibodies, the nucleoprotein is highly conserved among various CCHFV strains and can produce antibody and T-cell mediated immunity. This makes it an attractive candidate for broad pan-CCHFV protection[25]. Also, recent studies have shown that NP antibodies can protect through TRIM21-dependent intracellular pathways even without any neutralizing activity, which highlights the importance of including this antigen in vaccine constructs[26].

Modified Vaccinia Ankara vector platforms have shown great promise for developing CCHFV vaccines. A study published in March 2025 demonstrated that a prime-boost immunization strategy using nanospheres and MVA expressing the CCHFV nucleoprotein elicited broad immune responses in mice. This heterologous prime-boost method was more immunogenic than single-platform strategies[27]. Earlier studies also revealed that heterologous vaccination schedules combining adenoviral vectors with MVA induce the strongest CCHFV-specific cell-mediated and humoral antibody responses[17]. In addition, RNA-based vaccine technologies have also emerged as potential candidates; recent studies on mRNA vaccines expressing CCHFV glycoproteins have reported protective efficacy in mouse models, although the best antigen configuration is still under evaluation. While these diverse platforms demonstrate encouraging preclinical results, adenoviral vector systems offer distinct advantages that justify their prioritization for CCHFV vaccine development, including well-established Good Manufacturing Practices (GMP)-compatible manufacturing processes, superior thermal stability compared to mRNA platforms, proven single-dose immunogenicity, and extensive regulatory precedent from successful deployment in other infectious disease contexts[25,26].

Current development efforts for a vaccine against CCHF are marked by significant innovations as well as continuing challenges[7]. Several vaccine platforms have shown encouraging results in animals, but they are not yet ready to enter human clinical trials. Additional challenges include lack of standardized animal models, limited understanding of immune correlates of protection, and sporadic outbreaks of CCHF. However, recent advances in nonhuman primate models now provide additional tools for vaccine testing and help with translation into real-world clinical applications. Most importantly, this field has made a giant leap forward with the first-ever human clinical trial for a CCHF vaccine beginning in 2023; this is a major step toward translating positive preclinical data into human therapeutics[9,11,28].

Due to the urgent need for effective CCHFV vaccines and the positive results shown by adenoviral vector systems, this research thoroughly explored the feasibility of producing novel adenovirus-vectored CCHFV vaccine candidates and characterized the protective immune responses they elicit. Unlike previous studies that employed either chimpanzee adenoviral vectors (ChAdOx2) or single-antigen human AdV5 vectors, our study uniquely focuses on human AdV5 vectors expressing dual-antigen formulations (NP-P2A-Gc) alongside comprehensive multi-formulation strategies using both homologous and heterologous prime-boost regimens. The main goal of this study is to assess the immune response and preventive effectiveness of both same and different priming/boosting strategies using diverse new adenovirus vectored CCHFV proteins in mice.

Results

Design and construction of recombinant adenovirus vectors expressing CCHFV antigens

To develop adenovirus-vectored vaccine candidates against Crimean-Congo hemorrhagic fever virus, we engineered multiple recombinant human adenovirus serotype 5 constructs designed to express different viral antigens. The base HAdV5 genome was modified by deletion of the E1 and E3 regions to create replication-defective vectors. Four distinct expression cassettes were designed and inserted into the viral genome: AdV-NP-P2A-Gc construct expressing both the nucleocapsid protein and the Gc glycoprotein linked via a P2A self-cleaving peptide sequence; AdV-NP construct expressing CCHFV-NP alone; AdV-Gc construct expressing CCHFV-Gc alone; and AdV-GPC construct expressing the full glycoprotein precursor. Each expression cassette was flanked by the cytomegalovirus immediate-early promoter and the simian virus 40 polyadenylation signal to ensure robust transgene expression. These designs are schematically represented in Fig. 1A.

Protein expression confirmation by western blot analysis

To verify expression of CCHFV antigens from the recombinant adenovirus vectors, western blot analysis was performed on lysates from infected cells, as shown in Fig. 1B. Using mouse anti-nucleocapsid monoclonal antibody, a prominent band at approximately 55 kDa was detected in lanes 2 (AdV-NP lysate), 3 (AdV-NP lysate), 4 (AdV-NP-P2A-Gc lysate) (in blue frame) corresponding to the CCHFV NP protein. Probing with mouse anti-Gc monoclonal antibody revealed distinct banding patterns across lanes 7 (AdV-Gc lysate) and 8 (AdV-NP-P2A-Gc lysate). A prominent band at approximately 75 kDa was observed, consistent with the Gc glycoprotein. The undigested fusion protein (NP-P2A-Gc) was likewise observed in the HEK293 cells (highlighted by the green double-headed arrows in lanes 4 and 8 of Fig. 1B), indicating time-dependent digestion of the product. Gn refers to the mature glycoprotein N (40 kDa), and Pre-Gn refers to the glycoprotein precursor (120 kDa) in lane 10. The molecular weight markers ranged from 40 to 120 kDa, confirming the expected sizes of the expressed

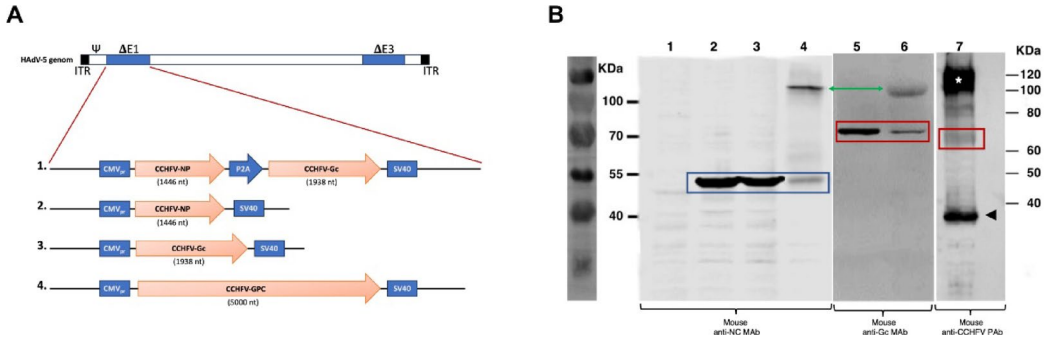


Fig. 1. Production and Characterization of Adenovirus-Vectored CCHFV Vaccine Candidates. This figure illustrates the design, expression, and physicochemical properties of the recombinant human adenovirus serotype 5 vectors expressing Crimean-Congo Hemorrhagic Fever Virus antigens. (**A**) Schematic representation of the HAdV5 genome, highlighting the E1 and E3 deletions for replication-deficiency. Four distinct vaccine constructs are shown: 1. AdV-NP-P2A-Gc, a dual-antigen vector expressing both nucleocapsid and Gc glycoprotein linked by a P2A sequence; 2. AdV-NP, expressing NP alone; 3. AdV-Gc, expressing Gc alone; and 4. AdV-GPC, expressing the full glycoprotein precursor. Each construct includes a cytomegalovirus immediate-early promoter and an SV40 polyadenylation signal. (**B**) Western blot analysis confirming the expression of CCHFV antigens in HEK293 cells infected with the recombinant adenoviruses. Lane1: HEK293 (uninfected control); Lane2: AdV-NP-Clone1; Lane3: AdV-NP-Clone2; Lane4 and 6: AdV-NP-P2A-Gc; Lane5: AdV- Gc; Lane7: AdV-GPC. Lanes 2,3,4 show expression of NP protein (blue frame at ~ 55 kDa) detected with mouse anti-NP monoclonal antibody. Lanes-5–6 show expression of Gc glycoprotein (red frame at ~ 75 kDa) detected with mouse anti-Gc MAb. Lane-7 shows expression of GPC and its processing products detected with mouse anti-CCHFV polyclonal antibody, revealing bands of PreGn (white asterisk at ~ 120 kDa), Gc (red frame at 75 kDa) and Gn (black arrowhead at ~ 40 kDa). Green arrow indicates undigested NP-P2A-Gc fusion protein of 130 kDa at lanes 4 and 8.

viral proteins. These results demonstrate successful expression of both NP and Gc proteins from the engineered adenovirus vectors.

Immunofluorescence confirmation of viral antigen expression in infected cells

To further characterize antigen expression and cellular localization, indirect immunofluorescence testing was performed on cells infected with each recombinant adenovirus construct (Suppl. Figure S1). AdV-NC-P2A-Gc-infected cells displayed robust green fluorescence throughout the cytoplasm, indicating widespread expression of both NP and Gc proteins. AdV-NP-infected cells similarly showed strong cytoplasmic green fluorescence, confirming NP protein expression. AdV-Gc-infected cells exhibited cytoplasmic green fluorescence with some concentration in perinuclear regions, which may be consistent with glycoprotein processing through the endoplasmic reticulum (ER) and Golgi apparatus, though additional subcellular localization studies would be needed to definitively confirm this trafficking pattern. AdV-GPC-infected cells demonstrated diffuse cytoplasmic fluorescence, indicating expression of the full glycoprotein precursor. DAPI counterstaining revealed intact nuclear morphology in all infected cells, and merged images confirmed that the antigen expression was predominantly cytoplasmic with no apparent cytopathic effects. The uniform and intense fluorescence signals across all constructs confirmed efficient transgene expression and validated the functionality of the recombinant adenovirus vectors.

Viral titer determination and purification efficiency

Following large-scale production and purification, viral titers were quantified at two stages of the purification process. Post-upstream process titers, measured after initial viral amplification and cell lysis but before chromatographic purification, ranged from 6×10^{11} to 2×10^{12} viral particles. Post-downstream processing titers represent final concentrations after complete purification including chromatographic steps. The AdV5-NP-P2A-Gc construct achieved the highest upstream titer at 2×10^{12} VP, followed by AdV5-Gc at 6×10^{12} VP, AdV5-NP at 8×10^{11} VP, AdV5-GPC at 6×10^{11} VP, and empty AdV5 at 7×10^{11} VP. Post-downstream processing, final titers ranged from 5×10^{9} to 6×10^{12} VP. Notably, AdV5-Gc and AdV5-NP maintained high titers of 6×10^{12} VP and 6×10^{10} VP respectively, while AdV5-NP-P2A-Gc yielded 5×10^{10} VP, AdV5-M Seg produced 6×10^{9} VP, and empty AdV5 achieved 5×10^{9} VP. These titers were suitable for downstream vaccine formulation and immunization studies. Detailed viral titers at each stage of purification are provided in Table 1.

Protein concentration in purified viral stocks and vaccine formulation

Protein concentrations in the purified adenovirus preparations were determined by spectrophotometry. Concentrations ranged from 0.74 to 1.44 mg/ml. AdV5-NP showed the highest protein concentration at 1.44 mg/ml, followed by AdV5-GPC at 1.38 mg/ml, AdV5-NP-P2A-Gc at 1.21 mg/ml, wild-type AdV5 at 1.14 mg/ml, AdV5-Gc at 1.07 mg/ml, and CCHFV-Ank2 at 0.74 mg/ml. These protein concentrations, combined with the

Construct	Post-upstream (IFU/mL)	Post-downstream (IFU/mL)
AdV5-NP-P2A-Gc	2×10^{12}	5×10^{10}
AdV5-NP	8×10^{11}	6×10^{10}
AdV5-Gc	6×10^{11}	6×10^{12}
AdV5-GPC	6×10^{11}	6×10^{9}
AdV5 Empty	7×10^{11}	5×10^{9}

Table 1. Viral Titers (viral particles, VP) at purification stages.

Construct	Protein concentration (mg/mL)
AdV5-NP-P2A-Gc	1.21
AdV5-NP	1.44
AdV5-Gc	1.07
AdV5-GPC	1.38
Empty AdV5	1.14
CCHFV-Ank2	0.74

Table 2. Protein concentrations of purified viral stocks.

viral particle titers, enabled precise formulation of vaccine doses for the subsequent immunogenicity studies. The protein concentrations for each purified adenovirus preparation are summarized in Table 2.

The vaccine formulation buffer was designed based on established Good Manufacturing Practice (GMP) protocols to maintain viral stability and immunogenic properties. Each 1 ml of formulation contained Tris aminomethane (20 mM) as a buffering agent, NaCl (75 mM) for isotonicity, sucrose (10% w/v) as a cryoprotectant and stabilizer, magnesium chloride hexahydrate (1 mM) as a cofactor, EDTA disodium salt dehydrate (0.1 mM) as a chelating agent, Polysorbate 80 (0.01% v/v) as a surfactant to prevent viral aggregation, and ethanol 95% (0.25% v/v) as a preservative. The formulation was brought to final volume with double-distilled water. This optimized formulation ensured viral stability during storage and maintained immunogenic properties for in vivo administration.

Immunogenicity assessment of adenovirus 5-vectored CCHFV vaccines

Immunization schedule and assessment strategy

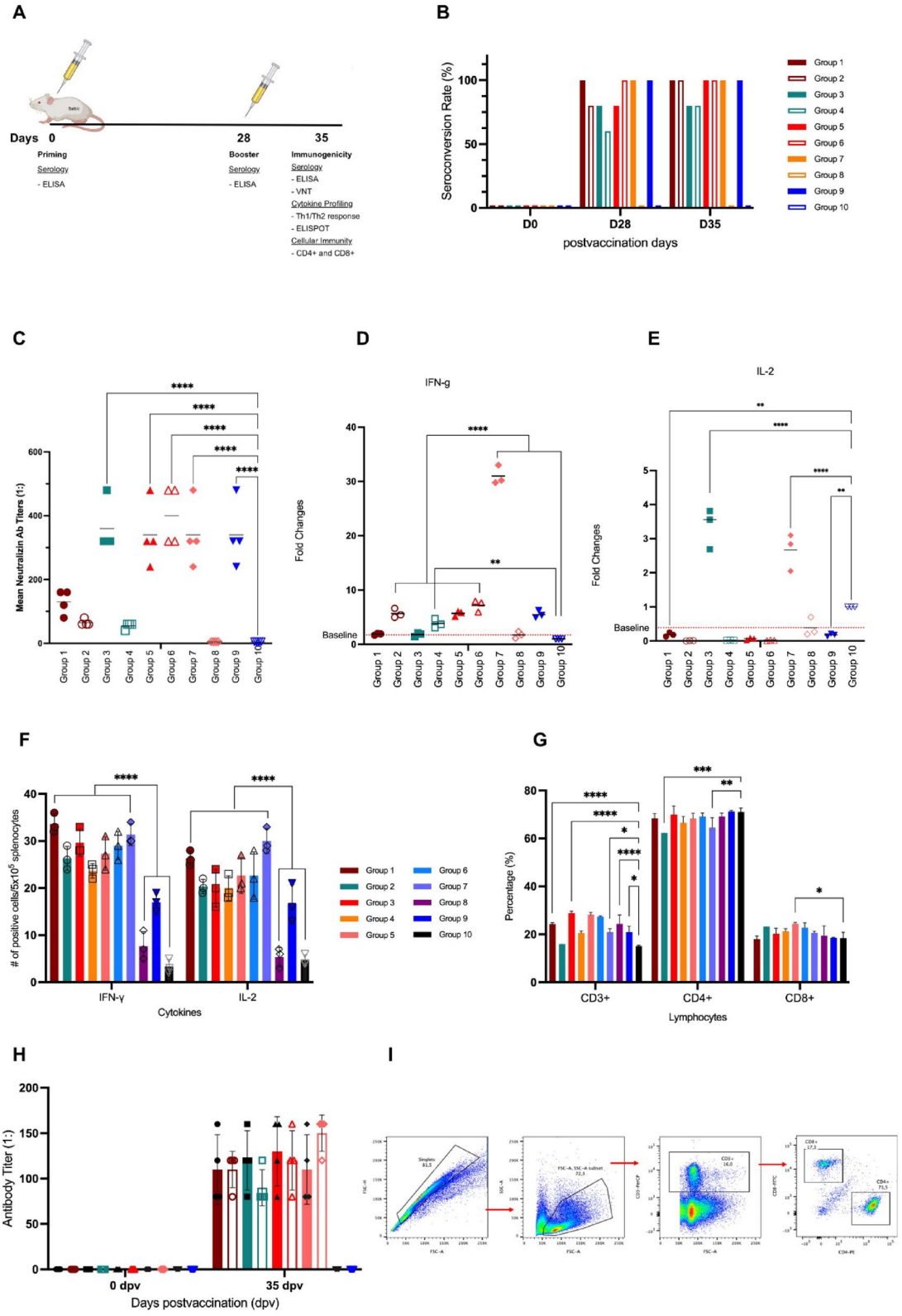
To comprehensively evaluate the immunogenicity of the adenovirus-vectored vaccine candidates, mice were immunized according to a homologous or heterologous prime-boost regimen[29]. The comprehensive immunization schedule and subsequent assessment strategy are detailed in Fig. 2A. Animals received a priming immunization on day 0, followed by serology assessment via ELISA at both days 0 and 28. A homologous booster immunization for Group 1, 6, 7, 8 and 9, and a heterologous booster immunization for Group 2, 3, 4, 5 (Table 3) were administered at day 28, with extensive immunogenicity profiling performed at day 35. The evaluation included serology (with ELISA), virus neutralization testing, cytokine profiling, assessment of Th1/Th2 responses, ELISPOT analysis, and cellular immunity characterization through CD4 + and CD8 + T cell phenotyping.

Kinetics of seroconversion following prime-boost immunization

Seroconversion rates were monitored at three time points: baseline (day 0), post-prime (day 28), and post-boost (day 35) across all experimental groups. At baseline, all groups showed 0% seroconversion as expected. Following the prime immunization, distinct seroconversion patterns were observed on day 28. Groups 1, 6, 7, and 9 exhibited 100% seroconversion, whereas seroconversion rates were 75% in Groups 2, 3, and 5 (3/4 animals), 50% in Group 4 (2/4 animals), and 0% in Groups 8 and 10. By day 35, one week after the homologous or heterologous booster immunization, most groups maintained or achieved 100% seroconversion rates, with Groups 1, 2, 5, 6, 7, and 9 showing complete seroconversion. Groups 3 and 4 demonstrated 75% seroconversion (3/4 animals), while Groups 8 and 10 remained at 0% (Fig. 2B). These kinetic data demonstrate that the adenovirus-vectored vaccines rapidly induce antibody responses after a single dose, with the booster immunization consolidating and enhancing these responses—though Groups 8 and 10, representing the empty Ad5 vector and naive control, respectively, failed to elicit any detectable response. The observed differences between seroconversion rates and neutralizing titers result from different assay sensitivities and targets: ELISA measures total anti-NC antibodies (including non-neutralizing), while virus neutralization tests measure functional antibodies against live virus (primarily targeting surface glycoproteins). Some animals may have low-level neutralizing antibodies that fall below the ELISA detection threshold for NC-specific antibodies, particularly in heterologous prime-boost groups where antigen presentation kinetics differ.

Neutralizing antibody titers following prime-boost immunization

Quantitative assessment of mean neutralizing antibody titers revealed robust humoral immune responses across vaccinated groups at day 35, as shown in Fig. 2C. Groups 3, 5, 6, 7 and 9 exhibited the highest mean neutralization



titers, ranging from 1:340 to 1:400 serum dilutions. Group 1 demonstrated intermediate titers (ranging between 1:80 and 1:160), while Groups 2 and 4 displayed the lowest antibody titers, means 1:65 and 1:55, respectively. Groups 8 and 10, representing the empty vector and naive control, exhibited zero titer. Statistical analysis revealed highly significant differences between high-responding vaccine groups (Groups 3, 5, 6 and 7) and empty AdV5 and vehicle groups (Groups 8 and 10) (****, $p < 0.0001$), indicating that specific antigen combinations and adjuvant formulations critically determine the magnitude of the neutralizing antibody response.

◀**Fig. 2**. Immunogenicity of Adenovirus-Vectored CCHFV Vaccines in Balb/c Mice Following Prime-Boost Immunization. This figure illustrates the humoral and cellular immune responses elicited by the various recombinant adenovirus vaccine candidates against CCHFV, as assessed through a prime-boost immunization regimen. (**A**) Schematic representation of the immunization and sampling schedule in Balb/c mice. Animals received a priming immunization on Day 0 and a booster immunization on Day 28. Serological assessments were conducted on Days 0, 28, and 35. Comprehensive immunogenicity profiling, including virus neutralization testing, cytokine profiling, ELISPOT, and cellular immunity characterization (CD4 + and CD8 + T cell phenotyping), was performed on Day 35. (**B**) Kinetics of seroconversion rates across all experimental groups at Day 0 (baseline), Day 28 (post-prime), and Day 35 (post-boost). Following prime immunization at Day 28, differential seroconversion patterns emerged, with most groups showing 80–100% seroconversion. By Day 35, most groups maintained or achieved 100% seroconversion rates. (**C**) Mean neutralizing antibody titers at Day 35 (post-boost) for each experimental group. Groups 1, 5, and 6 exhibited the highest mean neutralization titers, ranging from approximately 80 to 160 arbitrary units. Groups 9 and 10 showed the lowest neutralizing responses, with mean titers around 30–65 units. Statistical analysis revealed significant differences between groups, with Group 5 showing significantly higher neutralization titers compared to several other groups. (**D**) Fold changes in IFN-γ production (obtained from RTqPCR), a key marker of Th1-type cellular responses. Group 6 demonstrated the highest IFN-γ response with fold changes exceeding 30-fold compared to baseline. Group 6 showed highly significant differences compared to most other groups. (**E**) Fold changes in IL-2 production (obtained from RTqPCR), indicative of T cell activation and proliferative capacity. Groups 2 and 5 exhibited the highest IL-2 responses with fold changes reaching approximately 3.5–4.0-fold above baseline. Highly significant differences were observed between high-responding groups and most other groups, with additional significant differences between intermediate and low responders. (**F**) Comparative ELISpot analysis of IFN-γ and IL-2 production presented as percentages of responding splenocytes. Data represent cytokine-producing cells per total splenocytes analyzed from each experimental group. (**G**) Flow cytometric analysis of T cell subsets, displaying the percentages of CD3 + , CD4 + , and CD8 + lymphocytes. CD3 + T cell frequencies showed slight elevations in Groups 6, 7, 8, and 9 ($p < 0.0001$, $^{*}p < 0.05$). CD4 + T helper cells showed significantly elevated frequencies in Groups 4, 5, 6, 7, 8, and 9 ($^{***}p < 0.0001$, $^{***}p < 0.001$, $^{**}p < 0.01$). CD8 + cytotoxic T lymphocyte frequencies showed modest variation, with Groups 1, 9, and 10 showing slightly lower frequencies (around 15–20%) compared to others. (**H**) Kinetics of anti-adenovirus serotype 5 (AdV5) neutralizing antibody development in immunized BALB/c mice. Serum samples collected at baseline (day 0) and post-boost (day 35) were assessed for neutralizing antibodies against the AdV5 vector using virus neutralization testing. Each symbol represents a different experimental group (corresponding to Groups 1–10 as defined in the main study), with individual data points shown and error bars indicating standard error of the mean. (**I**) Representative flow cytometry plots illustrating the systematic gating strategy employed for T cell subset analysis. Initial gating identified the total lymphocyte population, followed by singlet discrimination, and then identification of CD3 + T cells, which were further subdivided into CD4 + T helper and CD8 + T cytotoxic cells.

Group	Day 0 (dose)	Day 28 (dose)	Regimen type
1	AdV5-NP-P2A-Gc (10^7 VP)	AdV5-NP-P2A-Gc (10^7 VP)	Antigenically Homologous
2	AdV5-Gc (10^7 VP)	AdV5-GPC + AdV5-NP ($10^5 + 10^7$ VP)	Antigenically Heterologous
3	AdV5-GPC (10^7 VP)	AdV5-Gc + AdV5-NP ($10^5 + 10^7$ VP)	Antigenically Heterologous
4	AdV5-NP (10^7 VP)	AdV5-Gc (10^7 VP)	Antigenically Heterologous
5	AdV5-NP (10^7 VP)	AdV5-GPC (10^7 VP)	Antigenically Heterologous
6	AdV5-NP + AdV5-Gc ($10^5 + 10^7$ VP)	AdV5-NP + AdV5-Gc ($10^5 + 10^7$ VP)	Antigenically Homologous
7	AdV5-NP + AdV5-GPC ($10^5 + 10^7$ VP)	AdV5-NP + AdV5-GPC ($10^5 + 10^7$ VP)	Antigenically Homologous
8	AdV5 (10^7 VP)	AdV5 (10^7 VP)	Control
9	Inactivated CCHFV	Inactivated CCHFV	Control
10	Vehicle	Vehicle	Control

Table 3. Study groups and vaccine compositions. The table delineates the experimental design, specifying the composition of vaccine formulations administered to experimental groups and vehicle (Group 10) at two distinct time points. Groups 1, 6, and 7 were administered an antigenically homologous prime-boost vaccination regimen, while Groups 2, 3, 4, and 5 received a heterologous prime-boost vaccination regime. Group 8 and 9 received AdV5 constructs and inactivated CCHFV, respectively. The numbers in parentheses denote the quantity of adenovirus vectors bearing CCHFV immunogens in viral particles for each administration.

Neutralizing antibody titers against AdV5 vector

All experimental groups showed negligible anti-AdV5 immunity at baseline (day 0), confirming absence of pre-existing vector-specific immunity in the study animals. Following the immunizations, all vaccine groups developed robust and comparable anti-AdV5 neutralizing antibodies by day 35 (titers ranging 1:80–1:160),

indicating uniform vector exposure and immune recognition across all vaccine formulations (Fig. 2H). The consistent vector-specific immune responses validate successful vaccine delivery while confirming that differential CCHFV-specific outcomes observed in the study were due to antigen-specific factors rather than variations in vector delivery or recognition.

IFN-γ production and Th1-type cellular responses

To evaluate cell-mediated immunity, we quantified interferon-gamma (IFN-γ) production, a key marker of Th1-type responses (Fig. 2D) on day 35. Splenocytes were stimulated with heat-inactivated CCHFV Ank-2 antigens, and cytokine production was measured by ELISpot assay. Group 7 demonstrated the highest IFN-γ response, with fold changes exceeding 30-fold compared to baseline (stimulated splenocytes from vehicle inoculated animals), indicating robust Th1 polarization. Groups 1, 3, 8, and 10 showed minimal IFN-γ production with fold changes below 3-fold. Groups 2, 4, 5, 6, and 9 displayed intermediate responses ranging from 4 to 8-fold. Statistical comparisons revealed highly significant differences between Group 7 and most other groups, confirming that specific vaccine formulations preferentially induce Th1-biased cellular immunity, which is critical for antiviral defense.

IL-2 production and T cell proliferative responses

IL-2 production, indicative of T cell activation and proliferative capacity, exhibited distinct and heterogeneous patterns across experimental groups (Fig. 2E) on day 35. Group 3 demonstrated the most pronounced IL-2 response, with fold changes reaching approximately 4.0-fold above baseline (stimulated splenocytes from vehicle inoculated animals), indicating robust T cell priming and expansion. Group 7 displayed a moderate IL-2 response (~2.5–3.0-fold), suggesting intermediate activation. In contrast, Groups 1, 2, 4, 5, 6, 8, and 9 maintained low IL-2 levels, ranging from 1.0 to 2.0-fold above baseline, indicating minimal proliferation signals. Group 10 showed only a limited increase in IL-2 (~1.5-fold), consistent with its role as a naive control group. Statistical analysis revealed highly significant differences between Group 3 and most other groups, confirming that specific vaccine formulations uniquely drive strong IL-2-dependent T cell expansion. The lack of coordinated IL-2 induction in many groups suggests that while IFN-γ responses may be present, effective clonal expansion is not universally achieved.

Balanced IFN-γ and IL-2 expression profiles

Comparative analysis of IFN-γ and IL-2 production from separate ELISpot assays revealed distinct cytokine profiles characteristic of different vaccine formulations (Fig. 2F). Group 7 showed the most pronounced balanced profile, with approximately 32% of splenocytes producing IFN-γ and 31% producing IL-2, indicating strong polyfunctional Th1 immunity. Group 1 exhibited the highest IFN-γ dominance (~35%) with high IL-2 production (~29%), suggesting potent polyfunctionality. Group 3 displayed a Th1-skewed profile with high IFN-γ (~29%) and moderate IL-2 (~21%). Group 6 showed a moderately balanced profile (28% IFN-γ, 22% IL-2), but its IFN-γ production was significantly lower than Groups 1 and 7. Groups 8 and 10 exhibited minimal cytokine production (< 5% for both cytokines). Statistical analysis revealed highly significant differences between high cytokine-producing groups and controls, confirming that vaccine formulation critically determines the quality and magnitude of cytokine responses.

T cell subset distribution and lymphocyte activation

Flow cytometric immunophenotyping revealed differential expansion of T cell subsets following immunization (Fig. 2G). CD3 + T cell frequencies showed relatively consistent patterns across most groups, ranging from 20–30%, with slight elevations in Groups 6, 7, 8, and 9 ($p < 0.05$). CD4 + T helper cells were uniformly expanded across all immunized groups, constituting 65–72% of CD3 + T cells, indicating a strong Th-cell bias regardless of vaccine formulation. However, we note that true expansion cannot be claimed without baseline (day 0) measurements for comparison. No group exhibited low CD4 + frequencies (~25–35%) as previously suggested for 'control' groups. CD8 + cytotoxic T lymphocyte frequencies displayed more modest variation, with most groups maintaining 20–25% of CD3 + T cells, though Groups 1, 9, and 10 showed slightly lower frequencies around 15–20%. These data indicate that the adenovirus-vectored vaccines preferentially expand CD4 + T helper populations, which likely contribute to coordinated humoral and cellular immune responses.

Flow cytometric gating strategy and population identification

Representative flow cytometry plots demonstrate the systematic gating strategy employed for T cell subset analysis (Fig. 2I). The CD4 + T helper cells and CD8 + T cytotoxic cells revealed non-overlapping populations with minimal double-positive cells. Dot plot analysis confirmed clear separation of CD4 + and CD8 + subsets, with minimal double-positive cells. This gating strategy ensured accurate quantification of T cell subsets and validated the quality of the immunophenotyping data.

Vaccine efficacy following lethal CCHFV challenge

Challenge study design

To evaluate the protective efficacy of the adenovirus-vectored vaccine candidates, immunized IFNAR$^{-/-}$ mice were subjected to a lethal CCHFV challenge study. Following the immunization animals received a lethal dose of CCHFV on day 42 (14 days after boost on day 28). The challenge study design is further outlined within the immunization and sampling schedule presented in Fig. 3A. Serology was assessed by ELISA at days 0 and 28 to monitor antibody responses prior to challenge. Neutralizing antibody titers were measured by virus neutralization testing at day 35 immediately before challenge. Post-challenge, animals were monitored for

clinical signs and survival, with terminal bleeding performed at day 45 for necropsy, virological analysis, and assessment of viral loads in target organs.

Seroconversion capacity

Pre-challenge assessment of antibody responses by ELISA revealed variable seroconversion rates across experimental groups, as presented in Fig. 3B. Groups 1, 6, 7, and 9 demonstrated 100% seroconversion rates, indicating that all animals in these groups developed detectable CCHFV NP-specific antibodies. Groups 2, 3, and 5 showed 75% seroconversion (3/4 animals). Group 4 exhibited 50% seroconversion (2/4 animals). Groups 8 and 10, representing the empty Ad5 vector and naive control, respectively, showed negligible seroconversion (~2%). These results indicate that most vaccine formulations were capable of inducing antibody responses in IFNAR$^{-/-}$ mice, though with varying efficiency—and some formulations (e.g., Groups 8 and 10) failed, as expected, to elicit robust anti-CCHFV humoral immunity.

Neutralizing antibody titers

Quantification of mean neutralizing antibody titers at day 35 revealed pronounced heterogeneity in humoral immune responses across the experimental groups (Fig. 3C). Groups 1, 3, 5, and 6 exhibited substantial inter-individual variability, with titers ranging from 1:30 to 1:160 antibody titers. The remaining vaccine groups elicited individually more homogeneous antibody titers spanning 1:15–1:120, indicating variable immunogenicity among animals.

Group 3 elicited the highest neutralizing antibody response (mean 1:105), which was followed by Group 6 (mean 1:87.5) at day 28. Groups 1, 2, 5 and 7 revealed mild-to-high neutralizing antibody responses (means 1: 80, 1: 70, 1:75 and 1:85, respectively) at day 28 (Fig. 3C). Among the formulated vaccine groups, Group 4 displayed consistently lowest neutralizing antibody titers, with values restricted to mean 1:15. Groups 8 and 10 elicited no neutralizing antibody response following the scheduled vaccination.

The apparent discrepancy between seroconversion rates and neutralizing titers observed in some groups results from different assay sensitivities and targets. ELISA measures total anti-NC antibodies (including non-neutralizing), while virus neutralization tests measure functional antibodies against live virus (primarily targeting surface glycoproteins). Some animals may have low-level neutralizing antibodies that fall below the ELISA detection threshold for NC-specific antibodies, particularly in heterologous prime-boost groups where antigen presentation kinetics differ. Seroconversion was measured using ELISA against CCHFV nucleocapsid (NC) protein as the capture antigen, which is the standard approach for CCHFV serology.

Collectively, these data demonstrate that adenovirus-vectored CCHFV vaccine candidates induce highly heterogeneous neutralizing antibody responses, with humoral immunogenicity strongly influenced by antigen composition and formulation strategy.

Survival following lethal CCHFV challenge

Kaplan–Meier survival analysis demonstrated clear differences in protection among the experimental groups following lethal CCHFV challenge (Fig. 3D). Groups 8 and 10 exhibited no protective efficacy, as all animals in these groups succumbed to infection between days 7 and 10 post-challenge. In contrast, Groups 1, 2, 4, 5, 6, 7, and 9 maintained 100% survival throughout the 10-day observation period, indicating complete protection against lethal CCHFV infection. Group 3 also showed no mortality, although mild clinical signs were observed in approximately 3% of animals during the follow-up period.

Collectively, these findings demonstrate that specific adenovirus-vectored vaccine formulations can confer robust and, in several cases, complete protection against lethal CCHFV challenge.

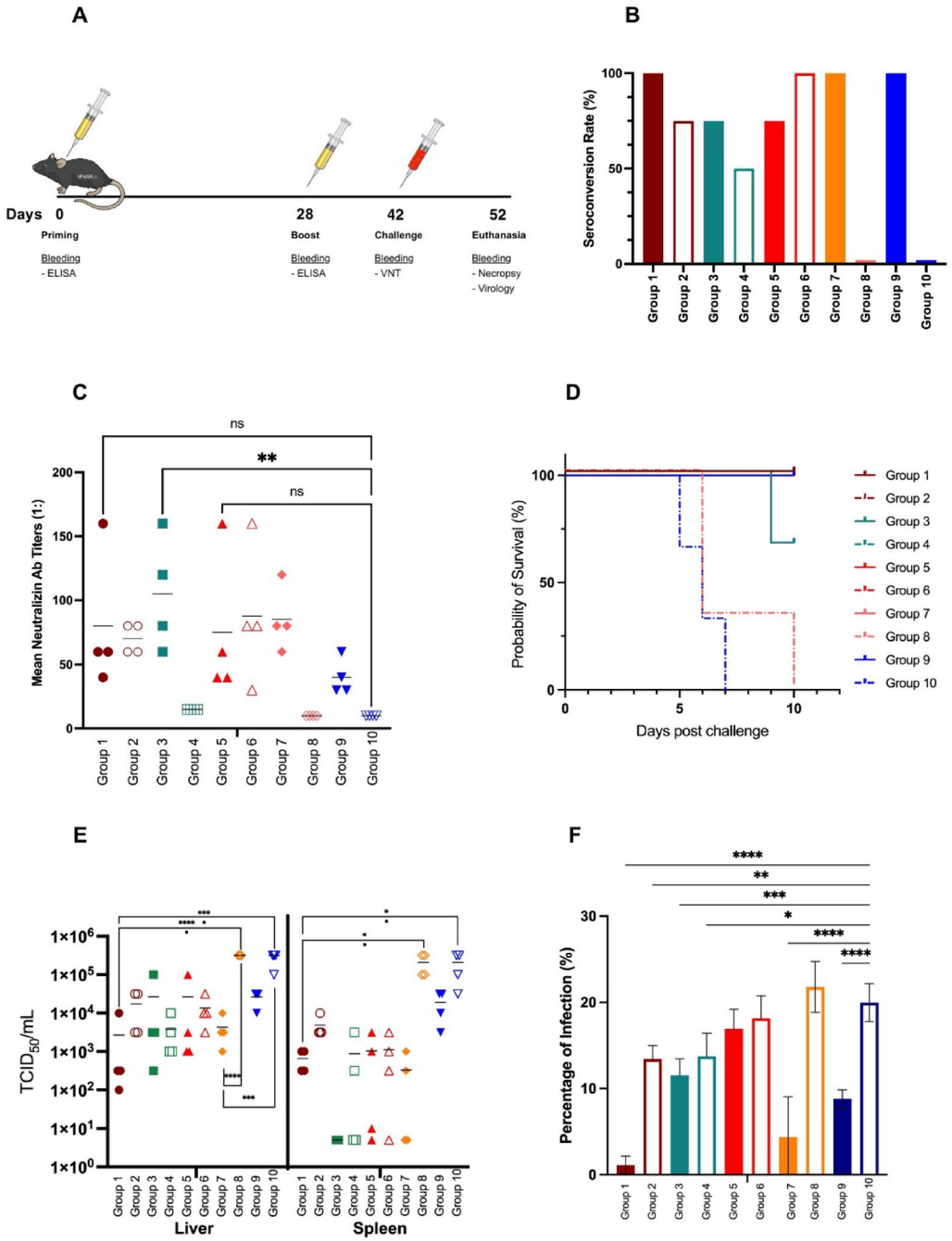
Viral load in target organs

Post-challenge viral replication and tissue dissemination were assessed by quantifying infectious viral loads in liver and spleen tissues on day 10 post-challenge (Fig. 3E). All vaccinated animals demonstrated significant viral load reduction of two to four logs in liver and spleen tissues, with some achieving complete clearance of the virus. In hepatic tissue, Group 10 (naive control) exhibited the highest viral titers, typically ranging from 10^4 to 10^6 $TCID_{50}$/mL, with several animals exceeding 10^5 $TCID_{50}$/mL, confirming uncontrolled viral replication. In contrast, Groups 1, 4, 5, 6, and 7 displayed consistently low hepatic viral loads (10^2–10^4 $TCID_{50}$/mL), representing a 2–4 log reduction compared to controls ($p < 0.001$ for Groups 1, 5, 6, and 7 vs. Group 10). Similarly, in spleen tissue, Groups 1, 4, 5, 6, and 7 maintained markedly lower titers (10^2–$10^{3.5}$ $TCID_{50}$/mL) compared to Group 10 (10^4–10^5 $TCID_{50}$/mL), representing a 1.5–3 log reduction ($p < 0.001$ for all comparisons vs. Group 10).

Groups 2, 3, 4, 5, 6, and 7 demonstrated heterogeneous yet overall reduced hepatic viral loads compared with the naive control group, indicating partial to substantial restriction of viral replication in the liver. Statistical analysis revealed significant differences among groups, supporting the conclusion that specific vaccine formulations effectively limited hepatic viral replication.

Analysis of splenic viral loads revealed a similar trend. Group 10 again exhibited the highest viral burden (10^4–10^5 $TCID_{50}$/mL), whereas Groups 1, 4, 5, 6 and 7 maintained markedly lower titers (10^2–$10^{3.5}$ $TCID_{50}$/mL) consistent with effective limitation of viral spread within lymphoid tissue. Notably, Group 3 displayed exceptionally low splenic viral loads (10^0–10^1 $TCID_{50}$/mL), indicating strong control of viral dissemination.

In contrast, Groups 8 and 9 exhibited higher residual splenic viral loads (Group 8: 10^4–$10^{5.5}$ $TCID_{50}$/mL; Group 9: 10^4–10^5 $TCID_{50}$/mL), in line with their comparatively weaker immunogenic profiles. Importantly, several animals in Groups 3, 4, 5, 6, and 7 showed complete viral clearance in spleen tissues, correlating with 100% survival and suggesting the induction of sterilizing immunity in a subset of vaccinated animals.



Immunohistochemical quantification of viral antigen in liver tissue

Further supporting the reduction in viral load, immunohistochemical analysis of liver tissues (Suppl. Figure S6) demonstrated decreased viral antigen presence. The mean percentages of CCHFV-infected hepatocyte areas in liver sections, quantified via AI-assisted analysis of individual data, are presented in Fig. 3F.

Collectively, the evaluation of neutralizing antibody responses, survival rates, and viral loads in target organs demonstrates that adenovirus-vectored vaccines encoding CCHFV antigens elicited protective immunity against lethal challenge, with their efficacy modulated by the specific antigen selected and the formulation approach. Furthermore, adenovirus monitoring in the same organs revealed no off-target spread of the vector, confirming its safety profile and reinforcing its potential as a CCHFV vaccine platform.

Discussion

This study successfully demonstrates the development, GMP-compatible production, and preclinical validation of adenovirus serotype 5-vectored vaccines expressing CCHFV antigens. Our findings establish that these vaccine candidates induce potent humoral and cellular immune responses conferring significant protection against lethal CCHFV challenge in murine models.

We successfully developed four distinct recombinant adenovirus serotype 5 constructs designed to express various CCHFV antigens: a bicistronic construct encoding NP-P2A-Gc, and three monocistronic constructs

◀**Fig. 3**. Protective Efficacy of Adenovirus-Vectored CCHFV Vaccine Candidates in IFNAR$^{-/-}$ Murine Models. This figure details the immunization regimen and subsequent assessment of immune responses and protection against lethal CCHFV challenge. (**A**) Schematic representation of the immunization and sampling schedule. IFNAR$^{-/-}$ mice received priming immunization on Day 0 and a booster on Day 28. Bleeding for ELISA was performed on Days 0, 28, and 42. Challenge with lethal CCHFV occurred on Day 42. Euthanasia, necropsy, and virological analysis were conducted on Day 45 (10 days post-challenge). (**B**) Seroconversion rates (%) at Day 42 (post-boost) for all experimental groups, indicating the proportion of mice that developed detectable antibodies. Groups 1, 6, 7, and 9 show 100% seroconversion, while other groups exhibit varying rates. (**C**) Mean neutralizing antibody titers at Day 42 (pre-challenge) for each experimental group. Groups 1, 2, 3, 5, 6 and 7 generally show higher neutralizing antibody levels compared to Groups 8, 9, and 10. Statistical significance (ns: not significant, $^{**}p < 0.01$) highlights differences between certain groups, such as Group 5 versus Group 8. (**D**) Kaplan-Meier survival curves illustrating the probability of survival (%) over 10 days post-lethal CCHFV challenge for all groups. Groups 1, 2, 4, 5, 6 and 7 demonstrate 100% survival, while Group 3 shows 75% survival. Control groups (Groups 8 and 10) showed 0% survival by days 7 and 10, respectively. (**E**) Quantification of CCHFV viral load in liver and spleen tissues at Day 52 (10 days post-challenge). Control animals show highest viral titers in both organs. Vaccinated groups, particularly those with higher survival rates, display significantly reduced or undetectable viral loads. Statistical analyses highlight significant reductions in viral load in several vaccinated groups compared to controls ($^{***}p < 0.001$, $^{****}p < 0.0001$). (**F**) Quantification of Immunohistochemistry Positive Areas in Liver Sections. This panel presents the mean percentages of CCHFV-infected hepatocyte areas within liver sections from different immunized and control mouse groups post-challenge, as determined by an AI-assisted analysis of individual data. Positive staining was defined as areas with pixel intensity ≥ 3-fold above background using the AI-assisted analysis platform. This quantitative assessment of viral antigen presence in liver tissue directly supports and complements the visual immunohistochemical findings detailed in Supplementary Figure S3. The minimal infected area was detected in Groups 1 and 7.

expressing NP, Gc, and GPC individually. Through Western blot and immunofluorescence analyses, robust expression of the target CCHFV proteins was confirmed, exhibiting their characteristic molecular weights and general cytoplasmic distribution. The glycoproteins showed concentration in perinuclear regions consistent with ER/Golgi processing, while the NP protein demonstrated diffuse cytoplasmic expression. The immunofluorescence analysis confirmed antigen expression and general cytoplasmic distribution; however, precise subcellular localization would require higher resolution confocal microscopy[30]. These rigorous characterization steps confirm the successful engineering of our adenoviral vectors, establishing a critical foundation for evaluating their immunogenicity and protective efficacy in vivo.

The downstream purification process yielded high-titer viral preparations suitable for vaccine formulation, with post-purification titers ranging from 5×10^9 to 6×10^{12} VP. Notably, the AdV5-NP-P2A-Gc construct achieved the highest upstream titer, suggesting that the bicistronic design did not compromise viral replication or productivity. The formulation buffer, incorporating stabilizers and cryoprotectants based on established GMP protocols, maintained viral stability while preserving immunogenic properties—a critical consideration for potential field deployment in CCHF-endemic regions with limited cold chain infrastructure[21].

The prime-boost immunization regimen induced rapid and robust immune responses across multiple experimental groups. Seroconversion was evident after a single dose in most groups, with rates reaching 75–100% by day 28, and was further enhanced following the booster dose at day 35. Cellular immune responses showed distinct patterns across vaccine formulations. Group 7 (2 × AdV-NP-GPC) demonstrated the most pronounced Th1 polarization, with IFN-γ production exceeding 30-fold over baseline. This dramatic expansion of CD4 + T cells and cytokine surge provides a mechanistic rationale for the superior protection observed; it suggests that the synergy between the conserved NP protein and the immunogenic Gc glycoprotein creates a broader "immunological net" than single-antigen strategies[5]. The coordinate induction of IFN-γ and IL-2 in several groups indicates effective T cell priming and expansion, with preferential expansion of CD4$^+$ T helper populations observed across most vaccinated groups.

Interestingly, Groups 3 (AdV-GPC + AdV-NP-Gc) and 7 (2 × AdV-NP-GPC) showed the highest IL-2 responses alongside moderate IFN-γ production, suggesting a more balanced Th1/Th2 response profile. This cytokine balance may be advantageous, as recent evidence suggests that both antibody-mediated and T cell-mediated mechanisms contribute to CCHFV immunity[31]. The flow cytometric analysis confirmed significant expansion of CD4$^+$ T cells, which likely supports both B cell help for antibody production and direct effector functions.

Pre-challenge assessment revealed variable neutralizing antibody responses, but high neutralization titers did not always correlate perfectly with complete protection, suggesting that other immune mechanisms contribute to vaccine efficacy. Correlation analysis between individual neutralizing antibody titers and survival outcomes revealed a weak positive correlation (Pearson $r = 0.23$, $p = 0.156$, $n = 35$ animals across vaccine groups), indicating that neutralizing antibody titers alone do not predict survival outcomes. This finding supports the hypothesis that protection against CCHFV operates through multiple immune mechanisms beyond neutralizing antibodies. This relationship aligns with recent findings demonstrating that anti-NP antibodies can provide protection through TRIM21-dependent intracellular mechanisms, independent of virus neutralization[31]. Groups other than 3, 8 (empty AdV) and, 10 (vehicle), achieved 100% survival despite showing moderate neutralization titers, while Group 3 (AdV-GPC + AdV NP-Gc) with higher neutralizing responses showed partial (75%) protection.

This disconnect between neutralizing antibody titers and protection outcomes aligns with recent findings by Leventhal et al. (2024) demonstrating that anti-NP antibodies can provide protection through tripartite motif-containing protein 21 (TRIM21)-dependent intracellular mechanisms, independent of virus neutralization[26,31]. While we did not directly investigate TRIM21-mediated protection in our study, our results support this emerging paradigm, as Groups 4 and 5, which showed complete protection despite moderate neutralization titers, received NP-containing formulations that would be expected to generate anti-NP antibodies[26]. Our results support the emerging paradigm that CCHFV vaccines should be evaluated based on survival and viral load reduction rather than neutralizing antibody titers alone. The 100% survival observed in Groups 4 (AdV-NP + AdV-Gc) and 5 (AdV-NP + AdV-GPC) demonstrates that complete protection against lethal CCHFV challenge is achievable with optimized vaccine formulations.

Groups showing partial protection still represent clinically meaningful outcomes, as reducing case fatality rates from 30% to under 10% would have substantial public health impact in endemic regions[32]. The mortality events in these groups occurred primarily between days 5–7 post-challenge, suggesting that a critical window exists during which immune responses must control viral replication to prevent lethal disease progression.

Post-challenge, viral replication and dissemination were evaluated by quantifying viral loads in liver and spleen tissues on day 10 post-challenge, utilizing assays. Within hepatic tissue, control animals from Group 10 (naive control), which experienced early mortality due to infection, exhibited elevated viral titers, typically ranging from 10^2 to 10^5, with several instances surpassing 10^5 $TCID_{50}$/mL. Conversely, Groups 2 (AdV-Gc + AdV-NP-GPC), 3 (AdV-GPC + AdV-NP-Gc), 4 (AdV-NP + AdV-Gc), 5 (AdV-NP + AdV-GPC), 6 (2 × AdV-NP-Gc), and 7 (2 × AdV-NP-GPC) presented with heterogeneous viral loads; the majority of animals in these groups maintained titers between 10 and 10^4 $TCID_{50}$/mL, while certain animals exhibited undetectable or remarkably low viral levels. Groups 8 (empty AdV), 9 (inactivated CCHFV), and 10 (vehicle) also displayed a spectrum of viral loads, ranging from 10^2 to 10^5 $TCID_{50}$/mL. Subsequent statistical analysis confirmed significant inter-group variations, specifically highlighting that several experimental groups achieved substantially reduced hepatic viral loads relative to the control group. In spleen tissue, vaccinated experimental groups displayed variable splenic viral loads ranging between 10^1 to $10^{3.5}$ $TCID_{50}$/mL. In control groups (Groups 8–10), higher mean residual viral loads ranging from $10^{4.5}$ to $10^{5.5}$ $TCID_{50}$/mL were detected. Significant differences were observed between groups, indicating that certain vaccine formulations effectively controlled viral replication in lymphoid tissues. Importantly, several animals from protected groups showed complete viral clearance in both liver and spleen, correlating with survival outcomes and suggesting sterilizing immunity in some cases. The variable viral loads observed among survivors within the same groups indicate individual variation in immune responses, a common feature in outbred populations that will be important to consider in clinical trial design. Control animals displayed high viral titers in both liver and spleen, confirming efficient viral replication and dissemination in the absence of immunity. The significant differences in organ viral loads between vaccinated and control groups provide quantitative evidence of vaccine efficacy beyond survival endpoints[31].

The 2-to-4 log reduction in viral loads within key organs provides quantitative evidence of efficacy beyond survival endpoints. The observation that several animals achieved complete viral clearance demonstrates the induction of sterilizing immunity in optimized groups. Furthermore, the absence of vector DNA in non-target tissues underscores a favorable safety profile, establishing a solid foundation for advancing these candidates toward Phase I clinical trials[33,34].

Our study design allowed direct comparison of single-antigen versus dual-antigen vaccination strategies. The bicistronic NP-P2A-Gc construct and the combination approaches all demonstrated strong immunogenicity and protection, supporting the rationale for dual-antigen vaccines. However, the monocistronic constructs also showed significant efficacy, with Groups 4 and 5 achieving 100% protection.

The superior performance of Group 7 (2 × AdV-NP-GPV) in inducing Th1 responses suggests that dose ratios and formulation strategies critically influence vaccine immunogenicity. This group received a lower dose of NP combined with standard Gc dose, which may have optimized antigen presentation and T cell priming. The finding that different antigen combinations and dose regimens achieve similar protection levels provides flexibility for vaccine development and suggests that multiple formulation strategies may be viable.

Recent studies have demonstrated that dual NP/GPC RNA vaccines provide complete protection in mice[26], and our results with adenoviral vectors expressing similar antigen combinations corroborate these findings using a different platform technology. The ability of both RNA and adenoviral platforms to achieve high-level protection when expressing both NP and glycoprotein antigens strengthens the case for multi-antigen vaccine approaches[24,35].

Our AdV5-vectored vaccines demonstrate comparable or superior efficacy to other platforms tested in similar models. ChAdOx2-vectored vaccines have shown promise in preclinical studies and advanced to Phase I clinical trials, representing the first CCHFV vaccine in human testing. Direct comparison of our results with published ChAdOx2 data reveals that our AdV5 platform achieved similar neutralizing antibody titers (80–400 AU vs. 100–320 AU for ChAdOx2) and superior survival outcomes (100% protection in 7/9 groups vs. 80–90% protection reported for ChAdOx2). While pre-existing immunity to AdV5 is more prevalent in human populations than to chimpanzee adenoviral vectors, our results demonstrate that the human AdV5 platform can still induce robust protective responses in animal models[17]. Our use of human AdV5 differs from the chimpanzee adenoviral platform, and while pre-existing immunity to AdV5 is more prevalent in human populations, our results demonstrate that this platform can still induce robust protective responses in animal models. Prior research has demonstrated that adenoviral vectors can generate efficient CD8 + T-cell memory even in individuals with pre-existing vector immunity, with these memory responses conferring protection upon viral challenge[36]. Furthermore, intranasal administration has shown efficacy against pre-existing immunity for adenovirus-based vaccines[37], and low levels of vector immunity (titer below 520 virus-neutralization units) did not compromise protective vaccine efficacy[38].

MVA-vectored approaches have also shown efficacy, particularly in heterologous prime-boost regimens with adenoviral vectors[17]. The recent demonstration that nanosphere/MVA prime-boost strategies elicit broad immune responses[27] suggests that our AdV5 vectors could similarly be combined with other platforms to enhance immunogenicity. DNA and RNA vaccine platforms have achieved protection in macaque models, often without detectable neutralizing antibodies, reinforcing the importance of cellular immunity that we observed in our studies[12,18,24,35].

The translation of our findings to human clinical trials will require careful consideration of several factors. First, the IFNAR$^{-/-}$ mouse model, while widely used and accepted for CCHFV research due to the requirement for interferon receptor knockout to achieve lethal infection, represents an immunocompromised system that may not fully recapitulate human immune responses. The absence of type I interferon signaling may alter the magnitude and kinetics of both innate and adaptive immune responses compared to immunocompetent hosts. However, this model has been extensively validated for CCHFV vaccine evaluation in the literature and provides a stringent test of protective efficacy. The recent development of nonhuman primate models provides an important bridging step, and our candidates should be evaluated in cynomolgus macaques before advancing to Phase I trials[18]. However, the recent development of nonhuman primate models provides an important bridging step[24], and our candidates should be evaluated in cynomolgus macaques before advancing to Phase I trials.

Second, pre-existing immunity to AdV5 exhibits significant geographical variance, with elevated seroprevalence frequently observed in African and Asian populations—regions where CCHF is endemic[39,40]. To circumvent this, alternative serotypes or heterologous prime-boost regimens are often proposed. The efficacy of AdV26-based COVID-19 vaccines illustrates the utility of using less common adenoviral serotypes in such populations[16,19]. However, diverging from the conventional preference for heterologous strategies, our findings indicate that a homologous regimen can provide enhanced robustness. We hypothesize that our specific 28-day dosing interval optimized antigen-specific priming while mitigating vector interference, which often plagues heterologous approaches like MVA-AdV5. This is supported by the uniform induction of anti-AdV5 neutralizing antibodies (titers 1:80–1:160) across all experimental groups, confirming consistent vector delivery. Consequently, the observed variations in CCHFV-specific protection are attributable to antigen-specific factors rather than disparities in vector uptake, aligning with evidence that vector immunity does not necessarily preclude effective transgene-specific responses[41,42]. These results suggest that a streamlined, single-platform schedule may offer high-level protection while avoiding the logistical hurdles of multi-platform systems.

Despite these promising results, certain limitations remain. First, our use of a homologous challenge (Ank-2 strain) necessitates further testing against heterologous genotypes to confirm cross-protection. Given the substantial genetic diversity among CCHFV strains across geographical regions, with the S segment (encoding NP) showing 20% nucleotide divergence and M segment (encoding glycoproteins) showing up to 31% divergence between genotypes, future studies should evaluate cross-protective efficacy against heterologous strains representing different genotypes. The high conservation of the NP protein across CCHFV genotypes (>80% amino acid identity) suggests that NP-containing vaccines may provide broader cross-protection than glycoprotein-only formulations, supporting our dual-antigen approach[3], future studies should evaluate cross-protective efficacy against heterologous strains representing different genotypes. The high conservation of the NP protein suggests that NP-containing vaccines may provide broader cross-protection than glycoprotein-only formulations[14,15]. Second, our study focused on systemic subcutaneous challenge rather than tick-bite transmission, which is the natural route of infection. While subcutaneous challenge is more relevant to nosocomial transmission and provides a stringent test of vaccine efficacy, evaluation against arthropod-borne challenge would strengthen the evidence base for vaccine deployment in endemic regions[43]. Third, while we demonstrate acute protection, long-term follow-up is required to assess the durability of these T-cell and antibody responses. Future studies employing systems immunology will be vital to pinpoint the exact correlates of protection that distinguish survivors from non-survivors. The recent demonstration that replicating RNA vaccines confer durable immunity against lethal CCHFV challenge in mice[25] suggests that our adenoviral vectors may similarly induce long-lasting protection, but this requires empirical validation.

Fourth, while we demonstrated significant protection and viral load reduction, the mechanisms underlying protection in survivors versus non-survivors within the same groups remain unclear. Future studies incorporating systems immunology approaches—including transcriptomics, proteomics, and detailed immune cell phenotyping—could identify correlates of protection and biomarkers predictive of vaccine response[29].

The successful completion of this preclinical efficacy study represents an important milestone, but substantial work remains before clinical translation. The WHO Blueprint for priority diseases emphasizes the urgent need for CCHFV vaccines[8,44], and the 2024 R&D roadmap specifically prioritizes vaccine development[9]. Our demonstration of GMP-compatible production processes, including optimized downstream purification using chromatographic methods, addresses a critical requirement for clinical-grade vaccine manufacture[21].

Regulatory pathways for CCHFV vaccine development face unique challenges due to the sporadic nature of outbreaks and ethical constraints on conducting traditional efficacy trials during epidemics[28]. The FDA Animal Rule provides a potential regulatory pathway allowing licensure based on efficacy in animal models when human trials are not ethical or feasible. Our study provides the type of robust efficacy data in well-characterized animal models that could support such an approach, particularly if corroborated by studies in nonhuman primate models[24].

Target populations for CCHFV vaccines include healthcare workers in endemic regions, veterinarians and agricultural workers with livestock exposure, laboratory personnel working with the virus, and military personnel deployed to endemic areas[4,9]. The cold chain requirements for our adenoviral vectors, while less stringent than mRNA vaccines, still represent a logistical consideration for deployment in resource-limited settings where CCHF burden is highest[20].

Beyond CCHFV specifically, our findings have implications for vaccine development against other bunyaviruses. The successful use of adenoviral vectors to express bunyavirus glycoproteins and nucleoproteins may inform vaccine strategies for related pathogens including Rift Valley fever virus, Hantaviruses, and emerging phleboviruses[10]. The demonstration that dual-antigen approaches can enhance protection suggests this strategy may be broadly applicable across the *Bunyavirales* order.

The observation that non-neutralizing antibodies targeting the nucleoprotein can contribute to protection through TRIM21-dependent mechanisms represents a paradigm shift in our understanding of antiviral immunity[31]. This mechanism may operate against other intracellular pathogens and suggests that vaccine antigen selection should consider targets beyond those eliciting neutralizing antibodies.

This study demonstrates that AdV5-vectored vaccines expressing CCHFV antigens induce robust humoral and cellular immune responses and provide significant to complete protection against lethal viral challenge in murine models. The successful GMP-compatible production process, comprehensive immunological characterization, and strong efficacy data support continued development of these vaccine candidates[11,29]. The achievement of 100% survival in optimized formulations, coupled with viral clearance in target organs, establishes proof-of-concept for adenoviral vector-based CCHFV vaccines.

Multiple formulation strategies showed efficacy, providing flexibility for clinical development and suggesting that both single-antigen and dual-antigen approaches merit further evaluation. The preferential induction of Th1 responses by certain formulations, combined with the generation of both neutralizing and non-neutralizing antibodies, indicates that these vaccines engage multiple protective immune mechanisms[25,26].

Moving forward, evaluation in nonhuman primate models, assessment of cross-protection against heterologous CCHFV strains, and studies of immune durability will be critical steps toward clinical translation[24,45]. The urgent public health need for CCHFV vaccines, highlighted by the WHO and demonstrated by ongoing outbreaks in endemic regions[2,9,32], underscores the importance of advancing promising candidates through the development pipeline. Our results contribute to the growing body of evidence supporting viral vector platforms for CCHFV vaccine development and bring us closer to addressing this critical unmet medical need.

Materials and methods

Ethical considerations and biosafety declaration

This study was conducted in accordance with the ARRIVE guidelines (https://arriveguidelines.org). All animal experimentation was approved by the Ankara University Animal Care and Use Committee (AUHADYEK; Approval #: 2022-13-125, dated July 06, 2022), and the research team adhered to the institutional and national guidelines for the care and use of laboratory animals throughout the study. Furthermore, all manipulations involving infectious Crimean-Congo Hemorrhagic Fever Virus were meticulously performed within Biosafety Level 3 and Animal Biosafety Level 3 laboratories, observing stringent adherence to institutional and national biosecurity protocols to safeguard both research personnel and the environment.

Virus and cell lines

The Crimean-Congo Hemorrhagic Fever Virus Ank-2 strain was utilized as both the genetic material source and the challenge virus in this investigation. The CCHFV-Ank-2 was isolated from blood of a hospitalized patient in 2017 and was genome-wide sequenced previously (GenBank Accession numbers: PV135957, PV135958, PV135959 for S, M and L segments, respectively). Propagation of CCHFV occurred in Vero E6 cells (VERO C1008 [Vero 76, clone E6, Vero E6]; ATCC CRL-1586, USA), which were sustained in Dulbecco's Eagle's Minimum Essential Medium (Gibco, Thermo Fisher Scientific, Waltham, MA, USA), augmented with 10% fetal bovine serum (Gibco, USA), 2 mM L-glutamine (Gibco, Thermo Fisher Scientific, Waltham, MA, USA), 100 U penicillin, and 0.1 mg/mL streptomycin (Gibco, Thermo Fisher Scientific, Waltham, MA, USA). Concurrently, Human Embryonic Kidney cells (HEK293; ATCC-CRL-1573, USA), were employed for the rescue of recombinant human adenovirus type 5, specifically engineered to express the CCHFV nucleoprotein, glycoprotein precursor, glycoprotein complex, and the bicistronic NP-P2A-Gc proteins. These HEK293 cells were cultured in Dulbecco's Minimum Essential Medium, supplemented with 10% FBS, 2 mM L-glutamine, 100 U penicillin, and 0.1 mg/mL streptomycin. All cell cultures were maintained at 37 °C with 5% CO_2 atmosphere.

The recombinant Human Adenoviruses and the Crimean-Congo Hemorrhagic Fever Virus working stock underwent propagation and subsequent titration in HEK293 and VeroE6 cells, respectively, followed by cryopreservation at − 80 °C until required for experimental use. All associated biological assays, encompassing virus cultivation, titration, and neutralization, alongside animal experiments involving infectious viral particles, were meticulously conducted within the Biosafety Level 3 Plus and Animal Biosafety Level 3 Plus facilities of the Virology Department, Veterinary Faculty of Ankara University, Turkiye.

Construction of recombinant adenoviruses

Replication-deficient recombinant human adenovirus type 5 vectors, designed to express Crimean-Congo Hemorrhagic Fever Virus antigens, were generated utilizing the AdMax™HI-IQ Kit J (Microbix Biosystems, Canada). Diverse vector strategies were implemented, encompassing bicistronic co-expression of NP-P2A-Gc and monocistronic expression of NP, GPC, and Gc of CCHFV proteins. Construction of the pDC516-NP-P2A-Gc cassette was achieved via the Gibson Assembly PCR method (New England Biolabs, Ipswich, MA, USA). Gene fragments encoding NP and Gc from the CCHFV Ank2 isolate were amplified using specific primer pairs and Phusion High-Fidelity DNA Polymerase (New England Biolabs, Ipswich, MA, USA). A 57-base pair P2A sequence was chemically synthesized. The pDC516 vector, pre-digested with SmaI FastDigest enzyme (Thermo Fisher Scientific, Waltham, MA, USA), was assembled with the respective inserts following the manufacturer's protocol. The Gibson Assembly reaction was conducted at 50 °C for 1 h, employing a 1:3 vector-to-insert molar ratio. Furthermore, monocistronic vectors expressing NP, Gc, and GPC proteins derived from CCHFV Ank2

isolates were also engineered. These recombinant plasmids were subsequently transformed into competent E. coli DH5α cells via heat shock. Transformants were cultured on LB agar plates supplemented with ampicillin. Colonies were screened using colony PCR with specific primer pairs. Positive clones were further confirmed by EcoRV restriction enzyme (Thermo Fisher Scientific, Waltham, MA, USA) digestion, which consistently yielded a 7728 bp product, indicative of the correct insert for each construct. In addition, rAdV5-GFP was also generated as a control, employing the same methodologies as described for the antigen-expressing constructs. Briefly, the GFP gene was amplified using primers given in table and Phusion High-Fidelity DNA Polymerase. Resulting PCR product was then ligated into the pDC516 vector digested with restriction endonuclease enzymes flanking GFP amplicon and subsequently transformed into competent E. coli DH5α cells as described before.

Replication-defective recombinant adenoviruses were generated by co-transfecting HEK293 cells with pDC516 transfer plasmids, containing cloned CCHFV gene/gene fragments, and the pBHGfrtΔE1 backbone adenovirus plasmid. This co-transfection was performed using the liposome-mediated method with Lipofectamine 3000 (Invitrogen, Carlsbad, CA, USA). Specifically, HEK293 cells were seeded into 6-well culture plates at a density of 2.3×10^5 cells/well in 2 mL of DMEM supplemented with 10% FBS. Following overnight incubation, cells underwent co-transfection with transfer and backbone plasmids, employing a 1:2 molar ratio of backbone-to-transfer plasmid, again via the liposome transfection method. Each well received a total of 5 µg of plasmids for transfection. The cytopathic effects of transfected cells were monitored daily post-transfection. Viruses were harvested 10–12 days post-transfection, at which point cytopathic effects, characterized by rounded and detached cells, were evident across 90% of the cell monolayer. Viral particles were subsequently harvested via freeze–thaw lysis, followed by centrifugation at $5000 \times g$ for 30 min. A sufficient titer of recombinant viruses was achieved after three rounds of passage in HEK293 cells. The recombinant viruses were titered in HEK293 cells using the Adeno-X™ Rapid Titer Kit (Takara Bio Inc., Japan). Additionally, Ad5-wt virus was generated through the transfection of the pFG140 vector into HEK293 cells. All recombinant and wild-type adenoviruses underwent Next-Generation Sequencing confirmation prior to Good Manufacturing Practice production. Post-infectivity titer determination, the viral stocks were cryopreserved at − 80 °C.

Purification of recombinant adenoviruses

An optimized downstream purification protocol was employed for five distinct recombinant adenovirus type 5 vectors, which were generated as part of this research, using HEK293 cell culture supernatant. HEK293 cells were cultured in 182 cm^2 submerged flasks and subsequently transduced with replication-deficient AdVs at a multiplicity of infection of 0.001. Upon completion of viral replication, cellular lysis was induced directly within the culture flask using 0.5% Tween™ 20 for a duration of 4 h. Simultaneously, a 20 U/mL Benzonase™ treatment was applied to fragment host cell DNA. Normal flow filtration was performed utilizing a sequential combination of ULTA™ 2 µm and 0.45 µm glass fiber filters. Chromatographic methodologies were subsequently employed for further purification within the laboratories of the TUSEB Aziz Sancar Research Center in Ankara. Concentration and buffer exchange were achieved via tangential flow filtration utilizing a hollow fiber filter with a nominal molecular weight cut-off of 300,000 Da, performed on ÄKTA™ flux 6 filtration systems (Cytiva, USA) with a 20 mM Tris buffer. Dynamic binding capacity was determined using an ÄKTA Avant 150 system equipped with 4.7 mL pre-packed HiTrap™ columns. The initial capture protocol was optimized employing Capto Q ImpRes resin (Cytiva, USA). Columns were equilibrated with a buffer comprising 20 mM Tris, 450 mM NaCl, and 2 mM $MgCl_2$. Sample loading proceeded at approximately 80% of the determined DBC. To mitigate co-elution of residual DNA with the viral particles, an additional washing step using 480 mM NaCl was incorporated, followed by elution with a linear gradient up to 570 mM NaCl. Capto Core 700 (Cytiva, USA) was subsequently utilized as a final polishing step. The material previously captured by the Capto Q ImpRes resin was loaded as the sample at a volume of 30 column volumes (Figure S5).

Western blot analysis

HEK293 cells, infected with individual recombinant adenoviruses, were lysed using RIPA buffer supplemented with a Halt protease inhibitor cocktail (Thermo Fisher Sci. Waltham, AM, USA). The resulting lysates were diluted with 4 × Laemmli buffer and β-mercaptoethanol, followed by denaturation through heating at 95 °C for 5 min. Samples were then separated by gel electrophoresis on 5–20% polyacrylamide gels, prior to electrotransfer onto PVDF membranes (BioRad, Thermo Fisher Scientific, Waltham, MA, USA) using a Transblot Turbo semi-dry transfer system (BioRad, Thermo Fisher Scientific, Waltham, MA, USA). Membranes were subsequently blocked with Blotting-grade Blocker (BioRad, Thermo Fisher Scientific, Waltham, MA, USA) and then incubated with anti-NP and anti-GPC monoclonal antibodies. Anti-NP and anti-Gc monoclonal antibodies were generated during doctoral research by the primary author and extensively characterized prior to use in this study[46]. The anti-NP monoclonal antibody (clone designation: CCHF-NP-4B7) demonstrates specific recognition of the 55 kDa CCHFV nucleoprotein with working dilution of 1:800. The anti-Gc monoclonal antibody (clone designation: CCHF-Gc-2D3) shows specific recognition of 75 kDa CCHFV Gc with working dilution of 1:400. Additionally, mouse polyclonal anti-CCHFV antibody (1:500) generated from hyperimmune sera of CCHFV-infected mice were incorporated into the analysis to provide broad-spectrum antigen recognition. All incubations were conducted for one hour at room temperature. Visualization of protein bands was achieved following a 10-min incubation in darkness with Clarity Max Western enhanced chemiluminescence substrate (BioRad, Thermo Fisher Scientific, Waltham, MA, USA) solution, and membranes were subsequently imaged using the ChemiDoc MP System (BioRad, Thermo Fisher Scientific, Waltham, MA, USA).

For publication preparation, high-resolution blot images showing complete membrane edges and full-length documentation were archived from all experiments. Preliminary figure cropping was performed intentionally during manuscript figure preparation to optimize visual clarity and reader focus on relevant protein bands within publication space constraints. Full-length blot images for all replicates, showing complete membrane

boundaries and edges, are provided in the Supplementary Information files (Suppl. Figure S2–S4) to ensure full compliance with Nature's digital image integrity policies. Membrane cutting (if performed) was carried out after antibody hybridization to maximize protein detection efficiency.

Indirect immunoflourescence assay

The indirect immunofluorescence assay was performed following a previously established protocol. Initially, cells were seeded in 96-well microplates and subsequently infected with recombinant adenoviruses expressing CCHFV antigens. These cells were then fixed with cold methanol, permeabilized and blocked using phosphate-buffered saline containing 1% bovine serum albumin. The cells were then incubated for 1 h at 37 °C with primary antibodies, including anti-NP (1:400) and anti-Gc (1:250) monoclonal antibodies, alongside anti-CCHFV polyclonal antibodies (1:200), which specifically target the CCHFV antigens. Following a washing step, Alexa flour488-conjugated secondary anti-mouse antibody (from goats, Invitrogen, USA; 1:1000 dilution) were applied to enable the visualization of antigen–antibody complexes. DAPI staining (1 µ/mL) was performed for 5 min to visualize cell nuclei. The test was evaluated by examining the cells with a fluorescence microscope (Zeiss Axio Observer, Germany), and images were captured at 400 × magnification using a digital camera with appropriate filter sets for FITC (488 nm excitation) and DAPI (358 nm excitation).

Adenovirus titration

Adenovirus titers were quantified using the Adeno-X™ Rapid Titer Kit (Takara Bio Inc., Japan), adhering to the manufacturer's specified protocol. Initially, healthy HEK293 cells were seeded into 12-well plates at a density of 5×10^5 cells per well in complete growth medium. Viral samples underwent ten-fold serial dilutions utilizing either phosphate-buffered saline or culture medium as the diluent. Subsequently, each viral dilution was dispensed into duplicate wells, followed by a 48-h incubation period at 37 °C in a 5% CO_2 atmosphere.

Post-incubation, the cell culture medium was aspirated, and cells were fixed with ice-cold 100% methanol at − 20 °C for 10 min. Following fixation, wells were gently rinsed three times with PBS supplemented with 1% bovine serum albumin. Infected cells were then detected via immunostaining, involving a 1-h incubation with a mouse anti-hexon antibody (1:500 dilution) at 37 °C, followed by three washes with PBS + 1% BSA. A rat anti-mouse HRP-conjugated secondary antibody (1:2000) was subsequently applied for 1 h at 37 °C. After three final washes, color development was initiated by applying DAB substrate working solution for 10 min at room temperature. Positive cells, characterized by brown/black staining, were enumerated microscopically within a minimum of three fields per well.

Viral titers, expressed as infectious units per milliliter, were calculated using the following formula: IFU/ml = where fields/well = 594 for 12-well plates at 200X total magnification. All measurements were conducted in duplicate to ensure accuracy. Furthermore, the total protein concentration in purified viral stocks was assessed using the Bradford protein assay method (BioRad, Thermo Fisher Scientific, Waltham, MA, USA) measuring absorbance at 595 nm using a spectrophotometer (SpectroStar Nano, MBG Labtech, Germany).

Animal experiments

Animal experiments were conducted in ten groups. Seven of these groups were designed as experimental and the remaining three groups were designed as control groups. Animal experiments were conducted using two phases: immunogenicity evaluation in Balb/c mice (obtained from Kobay Deney Hayvanlari Laboratuvari, Ankara, Turkiye) and protective efficacy assessment in $IFNAR^{-/-}$ mice (purchased from B&K Universal Ltd., Hull, East Yorkshire, UK). All animals were housed in individually ventilated cage systems with standard laboratory chow and water ad libitum. Environmental conditions were maintained at 20–24 °C with 12:12 h light/dark cycles. Each animal received intramuscular injections of 100 µl vaccine volume containing the specified viral particle doses (10^5 to 10^7 VP as indicated in Table 3) administered into the quadriceps muscle. The specific viral particle doses were: high-dose constructs (NP-P2A-Gc, NP, Gc, GPC) at 10^7 VP per injection, and low-dose NP constructs in combination groups at 10^5 VP per injection, as detailed in Table 1.

Immunogenicity studies were performed using 6–8 week old female Balb/c mice (weight: 18–22 g) obtained from Kobay Deney Hayvanlari Laboratuvari, Ankara Turkiye. For immunogenicity studies, ten experimental groups were established, each containing four Balb/c mice (aged 6–8 weeks, female, randomized by weight). Animals were randomly allocated to groups using a randomization table. All immunizations were administered intramuscularly in the quadriceps muscle using 26-gauge needles with a total volume of 100 µL per injection. Blood samples were collected via mandibular vein on days 0, 28, and 35. On day 35, prior to sacrifice by cervical dislocation, mice were deeply anesthetized via intraperitoneal injection of a ketamine (100 mg/kg) and xylazine (10 mg/kg) cocktail to ensure the absence of pain and distress during the procedure and splenocyte cells were immediately cultured from collected spleen tissue. These cells were subsequently analyzed using cytokine assays, intracellular cytokine staining, and flow cytometric cell counting to assess immune cell functionality.

Protective efficacy studies employed 6–8-week-old female type 1 interferon receptor knockout ($IFNAR^{-/-}$) mice (weight: 18–22 g) purchased from B&K Universal Ltd. (Marshall Bioresources, Hull, East Yorkshire, UK). The experimental methodology is delineated in Fig. 2. Animals, organized into groups of four, underwent priming, boosting and heterologous prime-boosting vaccinations at 28-day intervals, utilizing vaccine formulations specified by the group-specific protocols outlined in Table 1. Following a 14-day post-boost period (on day 42), all cohorts were challenged subcutaneously with the CCHFV Ank-2 strain at a dose of 1000 $TCID_{50}$ administered in the scruff area using 26-gauge needles. Daily monitoring for clinical signs including lethargy, hunched posture, ruffled fur, reduced activity, and body weight and temperature were recorded throughout the entire observation period. Necropsy, including documentation of gross pathological findings, was performed on animals that succumbed during the follow-up period or were humanely euthanized (as described for Balb/c mice) on day 10 post-challenge. Virological evaluations, encompassing RT-qPCR and viral infectivity assays,

were conducted on collected organ tissues and blood samples. For tissue samples cryopreserved at − 80 °C, viral genomic load was quantified using RT-qPCR, and viral infectivity was assessed[47]. In addition, to monitor vector AdV5 dissemination from the injection site, small group of animals were visualized daily in tissue samples were collected from various organs including the liver, spleen, and lungs at necropsy for quantitative PCR analysis, targeting adenovirus genomic DNA[48].

Serological examinations

Serologic controls after AdV-vectored vaccinations against CCHF were carried out using commercial ELISA (ID Screen® CCHF Double Antigen Multispecies ELISA, France) and VNT. ELISA was performed according to manufacturer's recommendations. Briefly, 30 µL of each serum sample taken from Balb/c and IFNAR$^{-/-}$ groups on days 0, 28 and 35, and on days 0 and 28, respectively, and provided controls were incubated in NP-coated plates for 45 min. After washing, an NP-peroxidase conjugate was added for 30 min to "bridge" the captured antibodies. The reaction was revealed using TMB substrate for 15 min and halted with a stop solution. Optical densities (OD) were recorded at 450 nm. The cutoff for seroconversion was set at 2.1-fold above the mean absorbance of negative control sera plus two standard deviations. VNT was employed to elucidate the neutralizing ability of the actively immunized animals. Actively immunized BALB/c and IFNAR$^{-/-}$ mice serum samples, on day 35 for the both groups, were heat-inactivated at 56 °C for 30 min in a water bath and then serially diluted in Dulbecco's Modified Eagle's medium and mixed with an equal volume of 100TCID$_{50}$ of the virus in duplicate. After 1 h of incubation at 37 °C, the serum–virus mixture was inoculated in 1-day-old VeroE6 cells. The lower limit for neutralization assays was 1:10 serum dilution with 50% neutralization as the endpoint.

In the second step serum samples were tested for human adenovirus serotype 5 neutralizing antibodies using a similar neutralization assay to evaluate the effect of pre-existing AdV antibodies on vaccine efficacy. The test was performed using adenovirus serotype 5 expressing GFP, where the reduction in GFP expression was quantified to determine neutralizing antibody titers.

Cytokine assay

The splenocyte from the immunized BALB/c mice were dispersed to 24-well plates at a concentration of 2.5×10^5 cells per well and were immediately infected with 10 moi of CCHFV Ank-2 strain. The infected cells were further incubated for 72 h at 37 °C and a 5% CO_2 atmosphere. As controls, we included naïve, and virus stimulated splenocytes from the negative controls. The culture supernatants were collected at 48 and 72 h of incubation and were stored at − 80 °C until further use. The measurement of the cytokines derived from the induced and splenocyte supernatants of the BALB/c and IFNAR$^{-/-}$ mice alongside the BALB/c splenocyte supernatants were performed using a LEGENDplex™ Mouse Th1/Th2 Cytokine Panel kit, as described by the manufacturer, using a CytoFLEX Flow Cytometer platform (Beckman Coulter, USA).

ELISpot

Antigen specific IFN-γ (Cat No: EL485) and IL-2 (Cat No: EL402) production by splenocytes was quantified through enzyme-linked immunosorbent spot assay (R&D Systems, USA) to further characterize the cell-mediated immune response. Spleen cells from immunized mice were isolated and stimulated ex vivo with inactivated CCHFV to induce cytokine production[12]. Following stimulation, the number of IFN-γ and IL-2 secreting cells was enumerated with microscopic examination.

Immunoprofiling splenocytes

Splenocytes isolated from immunized Balb/c mice were stimulated with specific CCHFV antigens or ionomycin. The stimulated cells were then labelled with anti-mouse CD3-PerCP, anti-mouse CD4-PE, and anti-mouse CD8-FITC. The analyses were performed with BD FACS Canto II Flow Cytometer (USA). The systematic gating strategy employed for T cell subset analysis included initial gating on forward scatter area versus side scatter area to identify the total lymphocyte population based on characteristic size and granularity. Singlet discrimination was performed using FSC-A versus FSC-H to exclude doublets. Within the singlet lymphocyte gate, CD3 + T cells were identified and further analyzed for CD4 and CD8 expression. The CD3 + population was subdivided into CD4 + T helper cells and CD8 + T cytotoxic cells.

CCHF viral load detection

Viral infectivity was assessed by inoculating Vero cell monolayers with diluted tissue homogenates or whole blood samples[49]. To do this, samples were serially diluted and plated onto Vero cells, with cytopathic effects monitored over a 7-day incubation period. The lower limit of detection was $10^{1.5}$ TCID$_{50}$/mL based on the serial dilution protocol and minimum cell monolayer requirements. The 50% tissue culture infectious dose was subsequently calculated using the Reed & Muench method to quantify viral titers in the samples[50]. For quantitative polymerase chain reaction analysis, RNA was extracted from collected liver and spleen samples using a commercial RNA isolation kit, and viral genomic load was determined using primer sets given in Table 4. The limit of detection for RT-qPCR was 10^2 copies/mL based on standard curve validation.

Adenovirus genome detection

This approach enabled the comprehensive assessment of vaccine candidate dissemination and potential off-target effects, critical for evaluating safety and efficacy. Detection of adenovirus genomic DNA was performed using quantitative PCR with specific primers targeting conserved regions of the adenovirus genome. This technique was used for the precise detection of viral vector distribution and persistence the organs sampled for CCHFV quantitation, thereby providing insights into the biodistribution kinetics of the adenoviral vaccine[51].

Primer code	Primer sequence (5′→3′)	Product size (bp)	Purpose of use
Clonning			
NP-F-Slice	GAATTCCCCGGGAGATCTAAGCTTGAGCGCGGCCGCCGATATCCATGGAAAACAAGATCGAGGTGAAC	1526	Production of NP-P2A-Gc gene cassette
NP-R-Slice	AGGCTGAAGTTAGTAGCGCGGCCGCGGATGATGTTGGCACTGG		
P2A-F	CCAGTGCCAACATCATCCGCGGCCGCGCTACTAACTTCAGCCTGCTGAAGCAAGCTGGAGACGTGGAGGAGAACCCTGGACCTCGCGGCCGCCCCCTGTTCCTGGATTCT	72	
P2A-R	AGAATCCAGGAACAGGGGGCGGCCGCGAGGTCCAGGGTTCTCCTCCACGTCTCCAGCTTGCTTCAGCAGGCTGAAGTTAGTAGCGCGGCCGCGGATGATGTTGGCACTGG		
Gc-F-Slice	AGGAGAACCCTGGACCTCGCGGCCGCCCCCTGTTCCTGGATTCT	2007	
Gc-R-Slice	ATAAACAAGTTGCTCGAAGTCGACGAGGCGGCCGCGGGCCCTCAGCCGATGTGTGTCTTG		
M seg-F	GTAACTATAACGGTCTAATACGACTCACTATAGGG	5000	Production of M segment (GPC)
M seg-R	ATTACCTCTTTCTCCTAGAAGGCACAGTCGAGG		
Gene and virus load detection			
NP-F	ATGGAAAACAAGATCGAGGT	1446	Colony PCR
NP-R	GATGATGTTGGCACTGGT		
Gc-F	CCCCTGTTCCTGGATTCT	1938	Colony PCR
Gc-R	GATGTGTGTCTTGGTGCT		
NP-F2	ATGTCCTTCCTCCACTTGAGA	125	SyberGreen PCR
NP-R2	GCTGAGCTGAAGGTTGATGTTC		
Gc-F2	ACAAAGAAGGTGGAAATCAGC	500	SyberGreen PCR
Gc-R2	GACGAAAGGGGCCAGAAA		
qPCR-F	GGACATAGGTTTCCGTGTCATTA	124	CCHF Viral load detection using RTqPCR
qPCR-R	TCCTTCTAATCATGTCTGACAGC		
qPCR-ProB	FAM-AGAACAACTTGCCAATTACCAACAGGC-BHQ1		
Adenovirus detection			
AdV5-F	GCCACCGAGACGTACTTCAGC	222	Investigation of Adv5 presence in tissues
AdV5-R	CAGCACGCCGCGGATGTCAA		

Table 4. Primer and probe sequences. This table lists the primer and probe sequences used in this study, including their product sizes and specific applications in cloning (for NP-P2A-Gc, M segment) and detection (for Colony PCR, SyberGreen PCR, CCHF viral load detection via RT-qPCR, and investigation of AdV5 presence in tissues). The underlined regions indicate in-frame homology sequences of the target clonning DNA.

Immunohistochemical staining

AI-assisted analysis of immunohistochemical staining was performed using the HC Threshold Analyzer-Standalone platform. Positive staining was defined as areas with pixel intensity ≥ 3-fold above background. The analysis involved automated threshold detection, color deconvolution to separate DAB-positive areas from hematoxylin counterstain, and quantification of positive staining as percentage of total tissue area.

Statistical analysis

Statistical analysis was performed using GraphPad Prism version 10.0 (GraphPad Software, San Diego, CA). Sample sizes were calculated based on pilot studies with $\alpha = 0.05$ and power = 80%. A minimum of 4 animals per group was used for immunogenicity studies and challenge experiments. Survival data were analyzed using Kaplan–Meier curves with log-rank (Mantel-Cox) test for group comparisons. For continuous variables including antibody titers, cytokine levels, and viral loads, one-way ANOVA followed by Tukey's multiple comparison test was used for multi-group comparisons. Data normality was assessed using the Shapiro–Wilk test. Non-normally distributed data were analyzed using the Kruskal–Wallis test followed by Dunn's multiple comparison test. Statistical significance was set at $p < 0.05$ with Bonferroni correction applied for multiple comparisons. Data are presented as mean ± standard error of the mean (SEM) unless otherwise indicated. All statistical tests were two-tailed. For the ELISpot analysis, fold-change calculations were performed by dividing post-immunization values by baseline values for each individual animal.

Data availability

The data that support the findings of this study are available from the corresponding authors, (Aykut Ozkul, Hakan Gurdal), upon reasonable request. The code generated for scoring IHC (HC Threshold Analyzer-Standalone) is available under restricted access on Zenodo (https://doi.org/10.5281/zenodo.17991977) the CC BY-NP-ND license. Access will be provided from the corresponding author upon reasonable request.

Received: 12 February 2026; Accepted: 18 June 2026
Published online: 11 September 2026

References

1. Frank, M. G., Weaver, G., Raabe, V., State of the Clinical Science Working Group of the National Emerging Pathogens, T. E. C. s. S. P. R., Network. Crimean Congo hemorrhagic fever virus for clinicians-virology, pathogenesis, and pathology. *Emerg. Infect. Dis.* **30**, 847–853. https://doi.org/10.3201/eid3005.231646 (2024).
2. Frank, M. G., Weaver, G., Raabe, V., State of the Clinical Science Working Group of the National Emerging Pathogens, T. E. C. s. S. P. R., Network. Crimean-Congo hemorrhagic fever virus for clinicians-epidemiology, clinical manifestations, and prevention. *Emerg. Infect. Dis.* **30**, 854–863. https://doi.org/10.3201/eid3005.231647 (2024).
3. Shahhosseini, N. et al. Crimean-congo hemorrhagic fever virus in Asia, Africa and Europe. *Microorganisms* https://doi.org/10.3390/microorganisms9091907 (2021).
4. Lorenzo Juanes, H. M. et al. Crimean-Congo hemorrhagic fever, Spain, 2013-2021. *Emerg. Infect. Dis.* **29**, 252–259. https://doi.org/10.3201/eid2902.220677 (2023).
5. Hawman, D. W. & Feldmann, H. Crimean-Congo haemorrhagic fever virus. *Nat. Rev. Microbiol.* **21**, 463–477. https://doi.org/10.1038/s41579-023-00871-9 (2023).
6. de la Fuente, J. et al. Interventions for the control of Crimean-Congo hemorrhagic fever and tick vectors. *NPJ Vaccines* **9**, 181. https://doi.org/10.1038/s41541-024-00970-5 (2024).
7. Ahata, B. & Akcapinar, G. B. CCHFV vaccine development, current challenges, limitations, and future directions. *Front. Immunol.* **14**, 1238882. https://doi.org/10.3389/fimmu.2023.1238882 (2023).
8. Mehand, M. S., Al-Shorbaji, F., Millett, P. & Murgue, B. The WHO R&D blueprint: 2018 review of emerging infectious diseases requiring urgent research and development efforts. *Antiviral Res.* **159**, 63–67. https://doi.org/10.1016/j.antiviral.2018.09.009 (2018).
9. Semper, A. E. et al. Research and product development for Crimean-Congo haemorrhagic fever: Priorities for 2024-30. *Lancet Infect. Dis.* **25**, e223–e234. https://doi.org/10.1016/S1473-3099(24)00656-X (2025).
10. Zivcec, M., Scholte, F., Spiropoulou, C., Spengler, J. & Bergeron, É. Molecular insights into Crimean-Congo hemorrhagic fever virus. *Viruses* **8**, 106. https://doi.org/10.3390/v8040106 (2016).
11. Tipih, T. & Burt, F. J. Crimean-Congo hemorrhagic fever virus: Advances in vaccine development. *BioRes. Open Access* **9**, 137–150. https://doi.org/10.1089/biores.2019.0057 (2020).
12. Farzani, T. A. et al. Immunological analysis of a CCHFV mRNA vaccine candidate in mouse models. *Vaccines* https://doi.org/10.3390/vaccines7030115 (2019).
13. Farzani, T. A. et al. Bovine herpesvirus type 4 (BoHV-4) vector delivering nucleocapsid protein of Crimean-Congo hemorrhagic fever virus induces comparable protective immunity against lethal challenge in IFNα/β/γR^{-}/$^{-}$ mice models. *Viruses* https://doi.org/10.3390/v11030237 (2019).
14. Santak, M. & Matic, Z. The role of nucleoprotein in immunity to human negative-stranded RNA viruses-not just another brick in the viral nucleocapsid. *Viruses* https://doi.org/10.3390/v14030521 (2022).
15. Zivcec, M. et al. Identification of broadly neutralizing monoclonal antibodies against Crimean-Congo hemorrhagic fever virus. *Antiviral Res.* **146**, 112–120. https://doi.org/10.1016/j.antiviral.2017.08.014 (2017).
16. Murala, M. S. T., Gairola, V., Sayedahmed, E. E. & Mittal, S. K. Next-generation adenoviral vector-based vaccines for severe acute respiratory syndrome coronavirus-2. *Vaccines (Basel)* https://doi.org/10.3390/vaccines13040406 (2025).
17. Saunders, J. E. et al. Adenoviral vectored vaccination protects against Crimean-Congo haemorrhagic fever disease in a lethal challenge model. *EBioMedicine* **90**, 104523. https://doi.org/10.1016/j.ebiom.2023.104523 (2023).
18. Farzani, T. A. et al. Co-delivery effect of CD24 on the immunogenicity and lethal challenge protection of a DNA vector expressing nucleocapsid protein of Crimean Congo hemorrhagic fever virus. *Viruses* https://doi.org/10.3390/v11010075 (2019).
19. Bos, R. et al. Ad26 vector-based COVID-19 vaccine encoding a prefusion-stabilized SARS-CoV-2 spike immunogen induces potent humoral and cellular immune responses. *NPJ Vaccines* **5**, 91. https://doi.org/10.1038/s41541-020-00243-x (2020).
20. Ewer, K. J. et al. T cell and antibody responses induced by a single dose of ChAdOx1 nCoV-19 (AZD1222) vaccine in a phase 1/2 clinical trial. *Nat. Med.* **27**, 270–278. https://doi.org/10.1038/s41591-020-01194-5 (2021).
21. Sallard, E., Zhang, W., Aydin, M., Schroer, K. & Ehrhardt, A. The adenovirus vector platform: Novel insights into rational vector design and lessons learned from the COVID-19 vaccine. *Viruses* https://doi.org/10.3390/v15010204 (2023).
22. Mendonca, S. A., Lorincz, R., Boucher, P. & Curiel, D. T. Adenoviral vector vaccine platforms in the SARS-CoV-2 pandemic. *NPJ Vaccines* **6**, 97. https://doi.org/10.1038/s41541-021-00356-x (2021).
23. Golden, J. W. et al. GP38-targeting monoclonal antibodies protect adult mice against lethal Crimean-Congo hemorrhagic fever virus infection. *Sci. Adv.* **5**, eaaw9535. https://doi.org/10.1126/sciadv.aaw9535 (2019).
24. Hawman, D. W. et al. A DNA-based vaccine protects against Crimean-Congo haemorrhagic fever virus disease in a Cynomolgus macaque model. *Nat. Microbiol.* **6**, 187–195. https://doi.org/10.1038/s41564-020-00815-6 (2021).
25. Leventhal, S. S. et al. Replicating RNA vaccine confers durable immunity against Crimean Congo hemorrhagic fever virus challenge in mice. *NPJ Vaccines* **9**, 249. https://doi.org/10.1038/s41541-024-01045-1 (2024).
26. Leventhal, S. S. et al. Single dose, dual antigen RNA vaccines protect against lethal Crimean-Congo haemorrhagic fever virus infection in mice. *EBioMedicine* **101**, 105017. https://doi.org/10.1016/j.ebiom.2024.105017 (2024).
27. Calvo-Pinilla, E. et al. Prime-boost vaccination based on nanospheres and MVA encoding the nucleoprotein of Crimean-Congo hemorrhagic fever virus elicits broad immune responses. *Vaccines* https://doi.org/10.3390/vaccines13030291 (2025).
28. Muzammil, K. et al. Recent advances in Crimean-Congo hemorrhagic fever virus detection, treatment, and vaccination: Overview of current status and challenges. *Biol. Proced.* **26**, 20. https://doi.org/10.1186/s12575-024-00244-3 (2024).
29. Tipih, T. et al. Single dose VSV-based vaccine protects mice against lethal heterologous Crimean-Congo hemorrhagic fever virus challenge. *NPJ Vaccines* **10**, 109. https://doi.org/10.1038/s41541-025-01164-3 (2025).
30. Dai, S. et al. Interactome profiling of Crimean-Congo hemorrhagic fever virus glycoproteins. *Nat. Commun.* **14**, 7365. https://doi.org/10.1038/s41467-023-43206-1 (2023).
31. Leventhal, S. S. et al. Antibodies targeting the Crimean-Congo Hemorrhagic Fever Virus nucleoprotein protect via TRIM21. *Nat. Commun.* **15**, 9236. https://doi.org/10.1038/s41467-024-53362-7 (2024).
32. Frank, M. G., Weaver, G., Raabe, V., State of the Clinical Science Working Group of the National Emerging Pathogens, T. E. C. s. S. P. R., Network. Crimean-Congo hemorrhagic fever virus for clinicians-diagnosis, clinical management, and therapeutics. *Emerg. Infect. Dis.* **30**, 864–873. https://doi.org/10.3201/eid3005.231648 (2024).
33. Monath, T. P. et al. Immunological correlates of protection afforded by PHV02 live, attenuated recombinant vesicular stomatitis virus vector vaccine against Nipah virus disease. *Front. Immunol.* **14**, 1216225. https://doi.org/10.3389/fimmu.2023.1216225 (2023).
34. Vinzon, S. E. et al. Cross-protection and cross-neutralization capacity of ancestral and VOC-matched SARS-CoV-2 adenoviral vector-based vaccines. *NPJ Vaccines* **8**, 149. https://doi.org/10.1038/s41541-023-00737-4 (2023).
35. Hawman, D. W. et al. Accelerated DNA vaccine regimen provides protection against Crimean-Congo hemorrhagic fever virus challenge in a macaque model. *Mol. Ther.* **31**, 387–397. https://doi.org/10.1016/j.ymthe.2022.09.016 (2023).

36. Sakurai, F., Tachibana, M. & Mizuguchi, H. Adenovirus vector-based vaccine for infectious diseases. *Drug Metab. Pharmacokinet* **42**, 100432. https://doi.org/10.1016/j.dmpk.2021.100432 (2022).
37. Tatsis, N. & Ertl, H. C. Adenoviruses as vaccine vectors. *Mol. Ther.* **10**, 616–629. https://doi.org/10.1016/j.ymthe.2004.07.013 (2004).
38. Provine, N. M. & Klenerman, P. Adenovirus vector and mRNA vaccines: Mechanisms regulating their immunogenicity. *Eur. J. Immunol.* **53**, e2250022. https://doi.org/10.1002/eji.202250022 (2023).
39. Alhashimi, M., Elkashif, A., Sayedahmed, E. E. & Mittal, S. K. Nonhuman adenoviral vector-based platforms and their utility in designing next generation of vaccines for infectious diseases. *Viruses* https://doi.org/10.3390/v13081493 (2021).
40. Khan, S. et al. Sequential use of Ad26-based vaccine regimens in NHP to induce immunity against different disease targets. *NPJ Vaccines* **7**, 146. https://doi.org/10.1038/s41541-022-00567-w (2022).
41. Hrycak, C. P., Windmann, S. & Bayer, W. Comparative evaluation of the vaccine efficacies of three adenovirus-based vector types in the Friend retrovirus infection model. *J. Virol.* https://doi.org/10.1128/jvi.01155-19 (2019).
42. Sayedahmed, E. E. et al. Longevity of adenovirus vector immunity in mice and its implications for vaccine efficacy. *Vaccine* **36**, 6744–6751. https://doi.org/10.1016/j.vaccine.2018.09.031 (2018).
43. de la Fuente, J., Sobrino, I. & Villar, M. Design and evaluation of vaccines for the control of the etiological agent of East Coast fever. *Parasites Vectors* **17**, 479. https://doi.org/10.1186/s13071-024-06517-w (2024).
44. Mehand, M. S. et al. World Health Organization methodology to prioritize emerging infectious diseases in need of research and development. *Emerg. Infect. Dis.* https://doi.org/10.3201/eid2409.171427 (2018).
45. Hawman, D. W. et al. SARS-CoV2 variant-specific replicating RNA vaccines protect from disease following challenge with heterologous variants of concern. *Elife* https://doi.org/10.7554/eLife.75537 (2022).
46. Hanifehnezhad, A. *Production and Characterization of Monoclonal Antibody against Crimean-Congo Hemorrhagic Fever Virus* PhD thesis, Ankara University, Graduate School for Health Sciences, (2022).
47. Dowall, S. D. et al. A Crimean-Congo hemorrhagic fever (CCHF) viral vaccine expressing nucleoprotein is immunogenic but fails to confer protection against lethal disease. *Hum. Vaccin. Immunother.* **12**, 519–527. https://doi.org/10.1080/21645515.2015.1078045 (2016).
48. Liu, J. et al. Heterologous prime-boost immunizations with chimpanzee adenoviral vectors elicit potent and protective immunity against SARS-CoV-2 infection. *Cell Discov.* **7**, 123. https://doi.org/10.1038/s41421-021-00360-4 (2021).
49. Borrego, B. et al. The Rift Valley fever (RVF) vaccine candidate 40Fp8 shows an extreme attenuation in IFNARKO mice following intranasal inoculation. *PLoS Negl. Trop. Dis.* **18**, e0012011. https://doi.org/10.1371/journal.pntd.0012011 (2024).
50. Leventhal, S. S. et al. Replicating RNA vaccination elicits an unexpected immune response that efficiently protects mice against lethal Crimean-Congo hemorrhagic fever virus challenge. *EBioMedicine* **82**, 104188. https://doi.org/10.1016/j.ebiom.2022.104188 (2022).
51. Doyle, J. D., Barbeau, D. J., Cartwright, H. N. & McElroy, A. K. Immune correlates of protection following Rift Valley fever virus vaccination. *NPJ Vaccines* **7**, 129. https://doi.org/10.1038/s41541-022-00551-4 (2022).

Author contributions

A.O., H.G., and S.O. conceptualized and designed the experiments. A.O., A.H., and S.O. created the dataset, while A.H., S.O., G.G.T., E.Y., E.T. and Y.T., conducted the experiments. A.O., A.H., S.O., G.G.T. and E.T. curated the data. A.O., M.T.K., N.U., A.B., A.K. and G.E. analyzed, validated, and interpreted the results. A.O. and A.H. wrote the original manuscript, and A.O., H.G., A.H., M.T.K., and Y.T. revised the paper. A.O., A.H. and S.O. developed and designed the interface. All contributors provided feedback on the text and discussed the findings.

Funding

This study received financial support from a grant provided by the Health Institutes of Türkiye (TUSEB) (Project No. 22897/28589).

Declarations

Competing interests

The authors declare no competing interests.

Additional information

Supplementary Information The online version contains supplementary material available at https://doi.org/10.1038/s41598-026-59094-6.

Correspondence and requests for materials should be addressed to H.G. or A.O.

Reprints and permissions information is available at www.nature.com/reprints.

Publisher's note Springer Nature remains neutral with regard to jurisdictional claims in published maps and institutional affiliations.

Open Access This article is licensed under a Creative Commons Attribution-NonCommercial-NoDerivatives 4.0 International License, which permits any non-commercial use, sharing, distribution and reproduction in any medium or format, as long as you give appropriate credit to the original author(s) and the source, provide a link to the Creative Commons licence, and indicate if you modified the licensed material. You do not have permission under this licence to share adapted material derived from this article or parts of it. The images or other third party material in this article are included in the article's Creative Commons licence, unless indicated otherwise in a credit line to the material. If material is not included in the article's Creative Commons licence and your intended use is not permitted by statutory regulation or exceeds the permitted use, you will need to obtain permission directly from the copyright holder. To view a copy of this licence, visit http://creativecommons.org/licenses/by-nc-nd/4.0/.

© The Author(s) 2026